MAPPING OF LINEAR GEOLOGIC STRUCTURES AT MOUNTAIN TOP UNIVERSITY'S PERMANENT SITE, MAKOGI-OBA, OGUN STATE, NIGERIA USING AEROMAGNETIC AND 2D ELECTRICAL RESISTIVITY TOMOGRAPHY DATA

Oluwatimilehin B. Balogun[1] (ORCID: 0000-0002-9287-2070), Daniel T. Joshua[1] and Elijah A. Ayolabi[1, 2].

Corresponding e-mail: obbalogun@mtu.edu.ng

[1] Department of Geosciences, Mountain Top University, Prayer City, Ogun State, Nigeria

[2] Department of Geosciences, University of Lagos, Akoka, Lagos State, Nigeria

Abstract

Aeromagnetic and 2D Electrical Resistivity Tomography (ERT) data have been processed, integrated and interpreted for the purpose of mapping linear geologic structures at Mountain Top University's permanent site in Makogi-Oba, Ibafo area of Ogun State which is currently being considered for development. The study was aimed at mapping linear geologic structures whose occurrences are to be given proper consideration in order to optimise land usage in the physical planning of the study area for development. The total magnetic field intensity (TMI) data were reduced to the magnetic equator to remove asymmetries associated with low magnetic latitude anomalies and was subsequently separated into its regional and residual field constituents. The residual field was enhanced using various techniques which included the Total Horizontal Derivative (THD), Standard Euler Deconvoluion and Tilt Derivative (TDR). Four 1110 m long 2D ERT profiles, probing a depth of about 220 m, were also acquired in the study area using the dipole-dipole array. The data were inverted using the "EarthImager^{TM}" software. The TMI map was observed to be dominated by elongated to linear magnetic anomalies trending mostly in the approximate N – S direction. Though having a low magnetic relief of about 2.6 nT, the study area reflected four magnetic field intensity zones which were characteristically distinct with magnetic intensity decreasing from West to East. The pattern of the decreasing magnetic intensities eastwards seemed to be suggestive of a step-faulting phenomenon with depth to the faulted blocks decreasing eastwards. The residual field map comprised of both elongated and spherical magnetic anomalies, some with relatively high magnetic intensities while others had relative low magnetic intensities. An intersection of magnetic lows in the eastern part of the study area was identified and interpreted to suggest that the study area is a shear zone. The lineaments delineated by the THD comprised of long, intermediate and short lineaments. From the THD map, the western and southern parts consist mostly of long and intermediate lineaments while the northeastern part was found to be dominated by short lineaments. The Euler Deconvolution mostly resolved long lineaments and their appendages but resolved less of isolated short lineaments. The integrated result of the THD and Euler deconvolution derived lineaments appreared to agree in a good part of the study area while in some parts it can be best described as complementary. From the Euler Deconvolution solutions, depth estimates to the linear geologic structures rarely exceeded 200 m except in the central southern and central northern parts. Tilt derivative solutions presented depths to some delineated semi-regional to regional scaled structures as ranging between 102.94 m and 286.76 m. The 2D ERT inverted section imaged three to four geoelectric layers which were interpreted as interclation of sand and clay. The immediate topsoil was found to be clayey and its thickness approached 8 m in some regions. Some structure suspected to be faults, coincident with the delineated magnetic lineaments, were imaged on the 2D ERT sections. The study area was

Preprint not peer reviewed

This preprint research paper has not been peer reviewed. Electronic copy available at: https://ssrn.com/abstract=4072454

found to be a shear zone having lots of linear geologic structures within it. The northwestern part of the study area appeared to be the least affected by the presence of linear geologic structures and may require less stabilisation for construction. The immediate topsoil being clayey, geotechnical competence tests may be required for the subgrade soil. Groundwater exploration should be concentrated around mapped faults, especially the ones identified on the 2D ERT sections. To optimize the groundwater resources in the area, the linear geologic structures which were all observed to dip towards the north on the 2D ERT profiles should be intersected at their direction of dip.

Keywords: Linear Geologic Structure, Total Magnetic Field Intensity, 2D Electrical Resistivity Tomography, Total Horizontal Derivative, Euler Deconvolution, Tilt Derivative.

Preprint not peer reviewed

This preprint research paper has not been peer reviewed. Electronic copy available at: https://ssrn.com/abstract=4072454

1. Introduction

Obtaining data about the subsurface either from the extrapolation of surface geological information or from direct measurement of physical properties of rocks and earth materials by geophysical methods is still the most potent fundamental means of deriving knowledge about structural disposition of an area (Reynolds, 2011; Parsekian *et al.,* 2015).

Various geophysical methods are often applied to solve specific geological problems especially when the nature of the study requires rapidity and less disturbance of the subsurface (Lowe and Zaccheo, 1991; O'Neil, 2001; Holden *et al.,* 2002; Rana, 2019). Geological problems often requiring geophysical solutions include exploration and mining studies, groundwater/hydrological studies, environmental and nuclear studies, and engineering site investigations and developmental planning (Fairbridge *et al.,* 1998; National Research Council, 2004; Gore and Davies, 2013).

Engineering site investigations and developmental planning is an aspect of geophysics, which though have been practiced for decades, is just gaining recognition and patronage in the developing economies of the world (Ribes and Finholt, 2009; Curtis and Low, 2016). It is gradually becoming obvious that modern civil engineering practices need information about the conditions of the subsurface (geologic information) as much as it needs accurate structural detailing which in time past has usually been its singular focus in order to maximise land resources (Walters, 2008; Griffiths and King, 2013; Dearman, 2013).

Some of the most effective geophysical methods for engineering site investigations and developmental planning include seismic refraction method (Cardarelli *et al.,* 2010; Adamo *et al.,* 2021), electrical methods (Oyedele and Olorode, 2010; Cardarelli *et al.,* 2010; Hossain *et al*., 2010), magnetic methods (Adagunodo *et al.,* 2015; Oyeniyi *et al.,* 2016; Balogun, 2019) and gravity method (McDowell *et al.,* 2002; Davis *et al.,* 2008) e.t.c.

Magnetic and electrical (electrical resistivity) methods remain two of the most patronised methods in engineering site investigation and developmental planning because of its affordable instrumentation and ease of use (Bogoslovsky and Ogilvy, 1997; Robinson *et al.,* 2008; Cardarelli *et al.,* 2010). Magnetic survey data often depict differences in the earth's magnetic field caused by the magnetic characteristics of the underlying rocks (e.g. magnetic susceptibilities). Magnetic susceptibility is lowest in sedimentary rocks, whereas it is highest in metamorphic and acidic

Preprint not peer reviewed

This preprint research paper has not been peer reviewed. Electronic copy available at: https://ssrn.com/abstract=4072454

igneous rocks, intermediate and basic igneous rocks (Telford *et al.,* 1990; Kearey *et al*., 2002). Magnetic survey can be land borne (ground magnetic survey), ship borne (ocean magnetic survey) or airborne (aeromagnetic survey) (Kearey *et al.,* 2002; Telford *et al.,* 1990; Reynolds, 1997).

Geologic zones of structural weaknesses (fracture and shear zones) can be delineated from aeromagnetic survey data (Udensi and Osazuwa, 2004; Balogun, 2019). Such zones of weakness have been known to be prospective hosts for a range of minerals. They are also indicators for exploring epigenetic, stress-related mineralization in rocks (Paterson and Reeves, 1985). They could as well serve as potential productive regions for groundwater abstraction (Oni *et al.,* 2020), however, their occurrence in large numbers and diverse orientations may render a place not suitable for construction purposes (Isaksson *et al*, 2017; Momoh *et al.,* 2008).

Electrical resistivity is a useful and reliable technique widely used in engineering site investigations to locate faults and fissures, sub-surface cavities, delineate permafrost and thaw zones, locate mineshafts and evaluate relative competence of soil layers in-situ (Griffiths and King, 2013).

One of the most significant pieces of information needed for planning in pre-construction site study, where geophysics has grown into a reliable, fast, cost-effective, and non-invasive tool, is the knowledge of the orientation, distribution, and depth extent of linear geologic features which include fractures and rock contacts (Isaksson *et al*, 2017). In most situations where pre-construction site research studies were deemed superfluous, avoidable structural flaws were discovered, and a large amount of money would have been squandered at this point (Mattsson and Wahlgren, 2010). As a result, major construction companies have begin to spend in pre-construction studies that include geophysical mapping of linear geologic features, many of which could be harmful to engineering constructions. The benefit of such pre-construction mapping is that resources are conserved, land is effectively utilized, engineering buildings are guaranteed to be durable, and human lives are not put at risk.

In line with this evolving good practice of pre-construction site investigation consisting of various geophysical methods for mapping linear geologic structures that could pose threats to civil engineering structures, Mountain Top University's permanent site at Makogi-Oba, Ibafo area of Ogun State was investigated for potential linear geologic structures that could be inimical to engineering structures using aeromagnetic and 2D electrical resistivity tomography data. The

Preprint not peer reviewed

This preprint research paper has not been peer reviewed. Electronic copy available at: https://ssrn.com/abstract=4072454

result of the investigation is expected to provide information that will guide choice of construction sites and recommend proper mitigation plans in areas where inimical geologic structures are unavoidable.

1.1 Description of the Study Area

The study area is the entire Mountain Top University's permanent site in Makogi-Oba community, off Lagos-Ibadan Expressway, Ibafo area, Ogun State, Nigeria. With reference to the WGS'84 datum, the area falls between Latitudes 06.7365^{o} N and 06.7513^{o} N; and Longitudes 03.3766^{o} E and 03.3911^{o} E. Expressed in Universal Transverse Mercator (UTM) coordinates with reference to WGS84 datum, the area is delimited by Latitudes 744640 and 746280 mN; and Longitudes 541620 and 543225 mE. Figure 1 is the location map of the study area.

1.2 Relief, Climate and Vegetation

From the elevation map of the study area (Figure 2), the study area can best be described as comprising significantly of low-lying areas flanked to the east, southwest and northwest by elevated portions. Having the least and maximum elevations as 6.2 and 22.7 m respectively, the relief is computed as 16.5 m. The river draining the area is the seasonal River Ipamorisha which is a tributary of River Ogun whose main channel is located 5 km due east away. The study area is within the floodplains of the Ogun river.

The region experiences two climatic seasons which are the dry and wet seasons. The dry season spans from November to March, and the wet season from April to October (Adeleke and Leong, 1978). Available rainfall data shows that rain falls throughout the whole year but a noticeable sharp decrease is usually observed from November to March. Average rainfall is 1693 mm per year while average temperature is 27.0ºC (Climate-data.org).

Ibafo (Makogi-Oba) is a wetland region. The vegetation of Ibafo is very similar to the vegetation observed generally in Lagos State, Nigeria. Just as in Lagos State, the vegetation can be classified as a typical swamp forest consisting of freshwater regions/freshwater swamp forest (Lagos State Government, 2015). In the flood plain regions, only grasses tolerant of heavy water are present.

1.3 Regional Geology of the Study Area

Preprint not peer reviewed

This preprint research paper has not been peer reviewed. Electronic copy available at: https://ssrn.com/abstract=4072454

The study area is located in the western part of the Nigerian sector of Dahomey Basin. The basin has been said to have been formed as a result of the Mesozoic splitting of the South America and

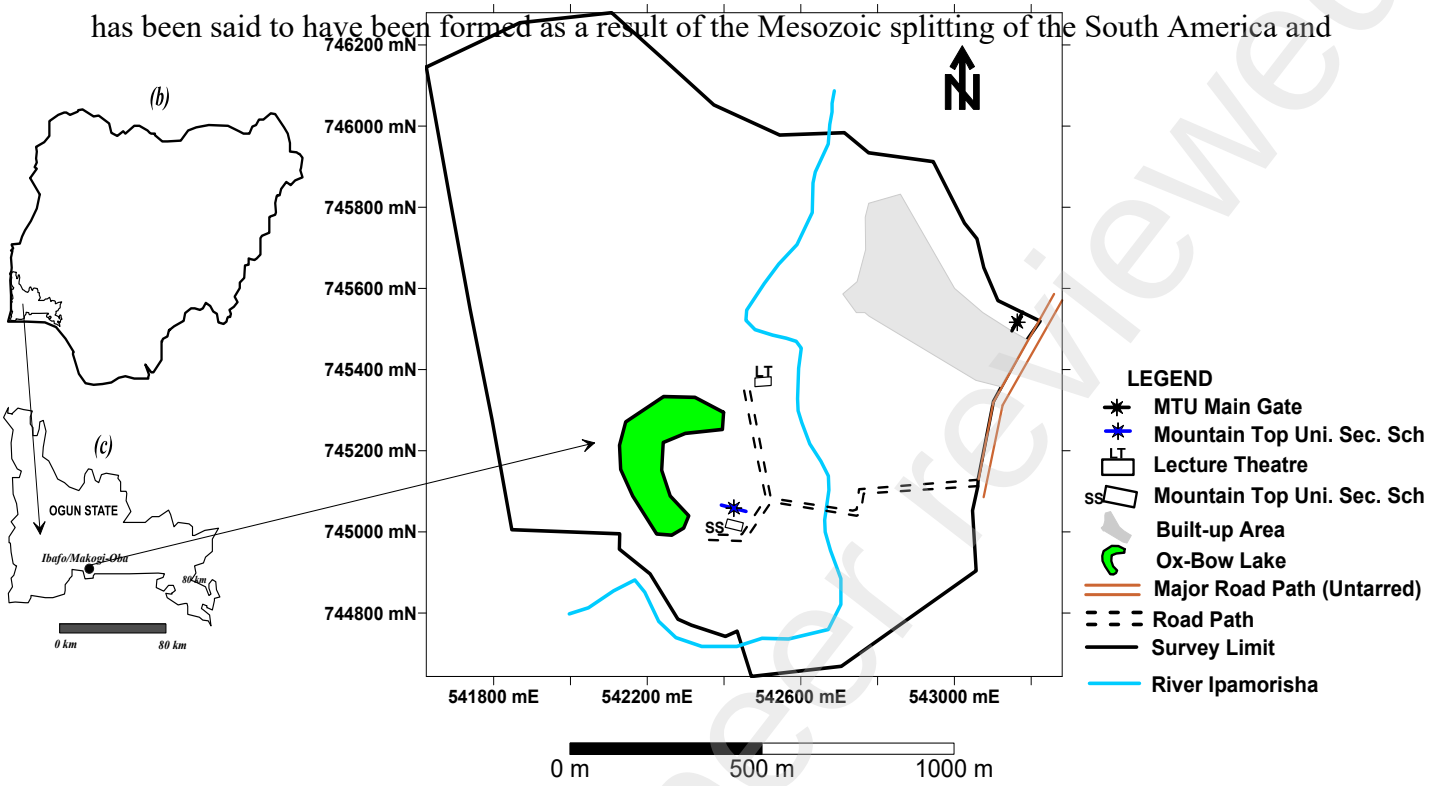

Figure 1: Location Map of the Study Area (*Digitised after Google Maps, 2021*)

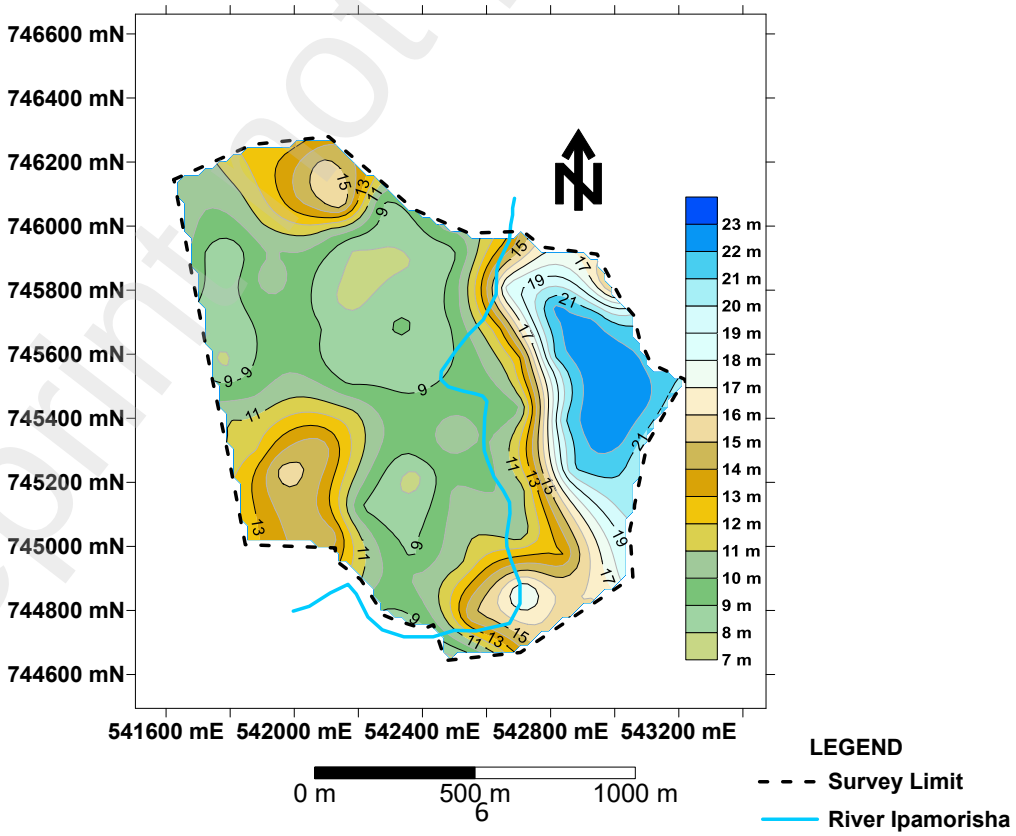

Preprint not peer reviewed

This preprint research paper has not been peer reviewed. Electronic copy available at: https://ssrn.com/abstract=4072454

Figure 2: Elevation Map of the Study Area (*Obtained from SRTM (USGS, 2006)*)

Africa plates (De Klasz and Du Chene, 1978). Non-fossiliferous folded rocks of unknown thickness but of pre-Albian (early Cretaceous) age, are the oldest deposits in the basin. Pleistocene through Recent strata are the youngest deposits. Omatsola and Adegoke (1981) ascribed the Cretaceous strata to the Abeokuta Group and grouped them into three formations: the Ise Formation (oldest), the Afowo Formation, and the Araromi Formation (youngest). The Araromi Formation is overlain by the Ewekoro Formation, which is also overlain by the Oshosun Formation whose continuity is limited laterally. In terms of its localised geology, the study area lies within the Recent Alluvium region of the Nigerian sector of the Dahomey basin, southwestern Nigeria (Figure 3).

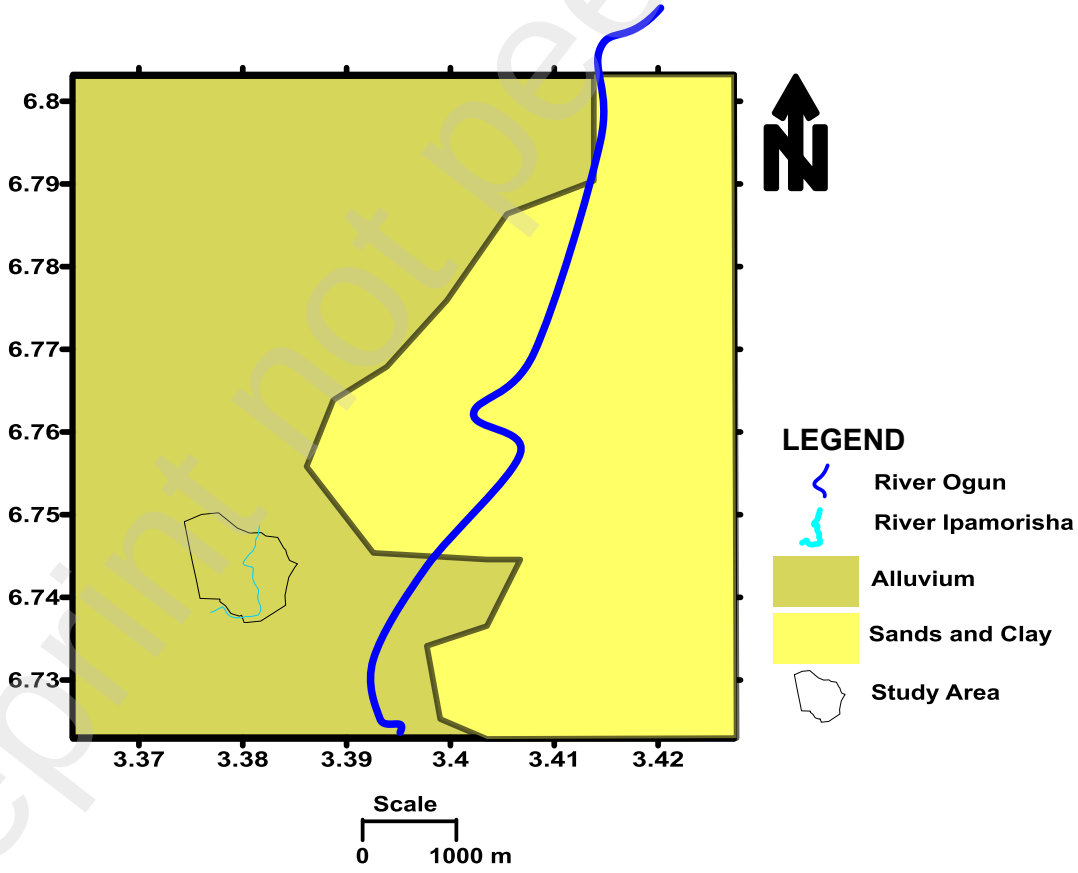

Preprint not peer reviewed

This preprint research paper has not been peer reviewed. Electronic copy available at: https://ssrn.com/abstract=4072454

Figure 3: Geologic Map of the Study Area (Digitized after Nigerian Geological Survey Agency, 2006).

2 Materials and Methods of Study

2.1 Materials

2.1.1 The Elevation Data

The elevation data adopted for the study is the high-resolution, Shuttle Radar Topographic Mission (SRTM) global elevation data (Digital Terrain Elevation Data – DTED®) having a spatial resolution of 30 m × 30 m and a near world-wide coverage. The data was acquired by radar interferometry and made use of the Earth's Gravity Model 1996 vertical datum. The unit of height measurement is metre (m) and the C-band wavelength is 5.6 cm. The elevation map generated from the elevation data has been presented in Figure 2.

2.1.2 The Aeromagnetic Data

The magnetic data used for the study is the high-resolution 100 m × 100 m grid aeromagnetic (Total Magnetic Field Intensity (TMI)) data, having a mean terrain clearance of 80 m and recording interval of 0.1 s, acquired by the Nigerian Geological Survey Agency between 2003 and 2010. For this study, the data was reduced to the magnetic equator to remove asymmetries associated with magnetic low-latitude anomalies. The regional field was removed and the resulting residual field was processed and analysed.

2.1.3 The 2D Electrical Resistivity Tomography (ERT) Data

Four 2D ERT lines were acquired from the western to central part of the study area as much as accessibility can allow. The lines were positioned to intercept lineament delineated from aeromagnetic data so that results from both the aeromagnetic data and 2D ERT can be integrated. The 2D ERT data was acquired using "SuperSting R8" earth resistivity meter which is a resistivity/IP meter, having 112 electrodes. The Dipole-Dipole array was used and the electrode spacing adopted was 10 m. The total spread length was 1110 m and the depth penetrated was 220 m. The 2D ERT data acquisition survey line plan is shown in Figure 4.

Preprint not peer reviewed

This preprint research paper has not been peer reviewed. Electronic copy available at: https://ssrn.com/abstract=4072454

2.2 Methods

2.2.1 Georeferencing and Digitisation the Analogue Site Map

The site map in form of an analogue survey plan was retrieved scanned, georeferenced and digitised. The coordinate system adopted in developing the analogue survey plan (i.e. UTM Zone 31N with reference to WGS84 Datum) was noted and was maintained while georeferencing and

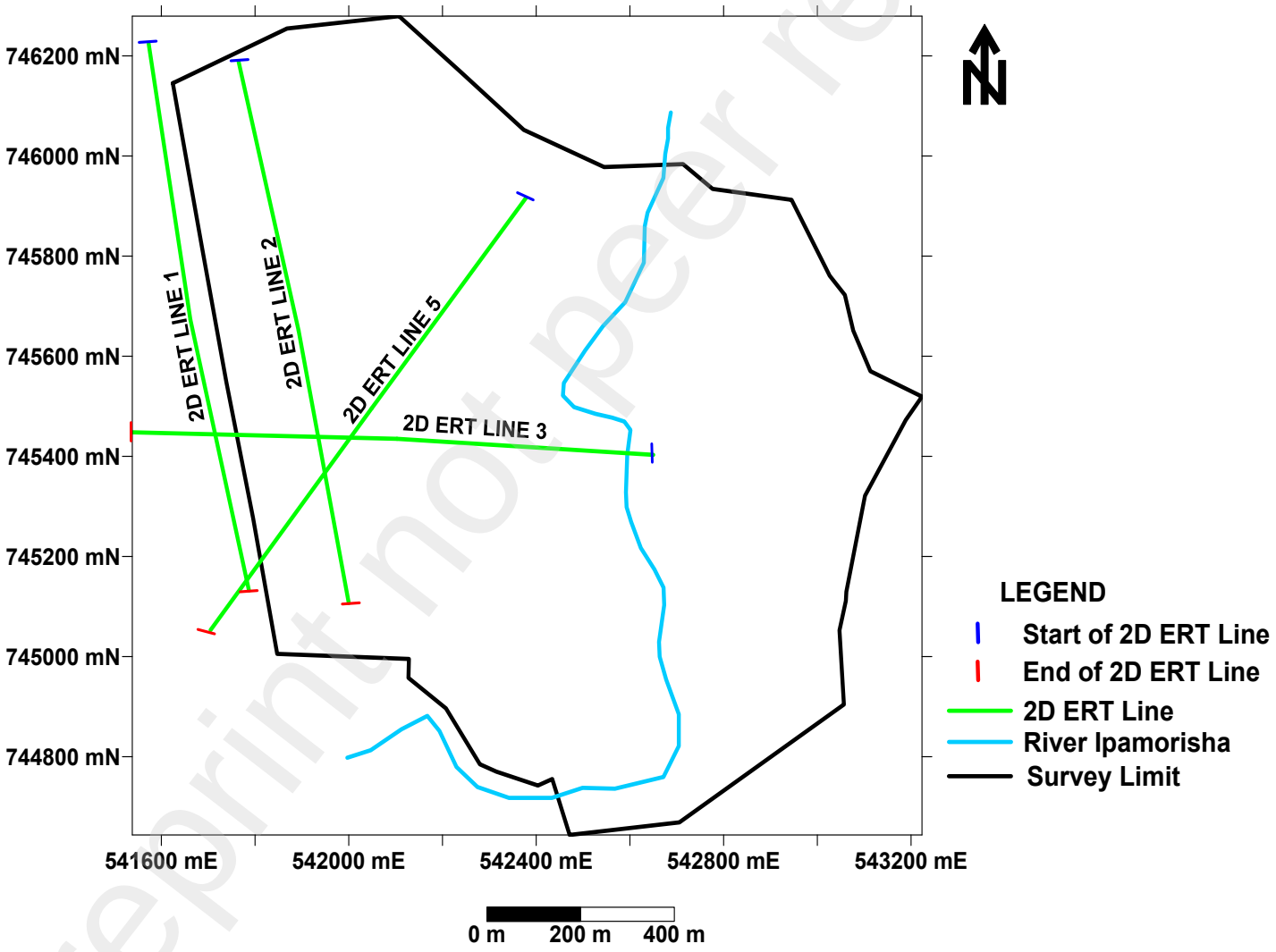

Figure 4: Base Map of the Study Area Showing the 2D ERT Profiles

Preprint not peer reviewed

This preprint research paper has not been peer reviewed. Electronic copy available at: https://ssrn.com/abstract=4072454

digitising the analogue map. The software used for both the georeferencing and digitisation is the Surfer Surface Mapping System Software, version 12.0.626 from Golden Software, Inc, Colorado, United States of America. Using the digitised values and coordinate system, a base map was developed for the study area (Figure 1).

2.2.2 Processing of the Aeromagnetic Data

The aeromagnetic data of the region where the study area is located (Sheet 279 – Ilaro Sheet) was procured from the Nigerian Geological Survey Agency (NGSA) and the study area was "windowed out" for localised processing operations. Near-surface (cultural) noises were first filtered using the upward continuation approach. The data were subsequently reduced to the magnetic equator using the "Reduction to the Magnetic Equator (RTE)" filter operator. This was done in order to reposition anomalies at magnetic low latitude to appear as if there were actually acquired at zero magnetic inclination so that interpretation will be less ambiguous.

The "Reduced to the Magnetic Equator" TMI data were decomposed into residual and regional field components using the least square polynomial fitting approach. The residual field was enhanced using the Total Horizontal Derivative (THD), Euler Deconvolution and Tilt Derivative (TDR) enhancement operations for proper delineation of the magnetic linear structures. The delineated lineaments were extracted and presented in as the magnetic lineament map. 2D Electrical Resistivity Tomography (ERT) data were subsequently acquired within the study area and the result integrated with the result of the magnetic data and interpreted. The software employed for the aeromagnetic data processing is the Geosoft's Oasis Montaj^{TM} software version 6.4.2 (HJ). The theories of the suites of basic data enhancement operations performed on the data are discussed below.

2.2.2.1 Least Square Polynomial Fitting

Preprint not peer reviewed

This preprint research paper has not been peer reviewed. Electronic copy available at: https://ssrn.com/abstract=4072454

This technique was first suggested for use for regional-residual field separation in potential field data processing by DeLury (1950) and was used by Oldham and Sutherland (1955). It was later modified by Grant (1957). The theory is summarized below.

Let the observed magnetic field T (x, y) be composed of a regional field T_R (x, y) and a residual field T_L (x, y) component.

Then

$$T(x, y) = T_R(x, y) + T_L(x, y) \quad (1)$$

Let T_L be a random variable with zero mean and constant variable σ^2. Let the observed anomaly T be expressed in terms of two orthogonal polynomials of degree p and q (i.e $f_p(x)$ and f_q (y)) so that

$$T(x, y) = a_{00}f_0(x)f_0(y) + a_{10}f_1(x)f_0(y) + a_{01}f_0(x)f_1(y) + \ldots + a_{pq}f_p(x)f_q(y) \quad (2)$$

where constant a_{rs} are determined by the least square techniques using the equation

$$a_{rs} = \frac{[s\{T(f_{r(x)})(f_s(y))\}}{S\{f_r^2(x)\}S\{f_r^2(y)\}} = \frac{T_{rs}}{p_r p_{s1}} \quad (3)$$

2.2.2.2 Total Horizontal Derivative

This is a very efficient operation, applicable to potential field data, commonly used to accentuate edges of structures. The principle is based on the fact that the gradient of a function will be peak at a discontinuous point. Therefore, when we differentiate a potential field function such as the gravity and magnetic fields, where the derivative is peak is usually representative of a discontinuous point or zone. The total horizontal derivative is given in equation 4 below as

$$THD = \sqrt{\left(\frac{\delta T}{\delta X}\right)^2 + \left(\frac{\delta T}{\delta y}\right)^2} \quad (4)$$

Preprint not peer reviewed

This preprint research paper has not been peer reviewed. Electronic copy available at: https://ssrn.com/abstract=4072454

Where $\frac{\delta T}{\delta X}$ is the derivative of the magnetic field in the "x: direction, and $\frac{\delta T}{\delta y}$ is the derivative of the magnetic field in the "y" direction.

2.2.2.3 The Euler Deconvolution

Euler deconvolution operation is a very efficient edge enhancement technique in potential field data processing. It is widely used because it requires only little prior information about anomaly source geometry and requires no information about anomaly source vector in the case of magnetic anomalies (Reid *et al.,* 1990; Balogun *et al.,* 2016; Balogun, 2019).

One major important advantage of Euler Deconvolution is that it gives the estimate of the depth of magnetic sources in addition to defining their edges. The Euler Deconvolution operation is based on solving Euler's homogeneity equation given in equations 5 and 6 as

$$(x- x_0)\frac{\delta T}{\delta \chi} + (y- y_0)\frac{\delta T}{\delta y} + (z- z_0)\frac{\delta T}{\delta z} = \eta\,(\beta - T) \qquad 5$$

$$x\frac{\delta T}{\delta \chi} + y\frac{\delta T}{\delta y} + z\frac{\delta T}{\delta z} + \eta T = x_0\frac{\delta T}{\delta \chi} + y_0\frac{\delta T}{\delta y} + z_0\frac{\delta T}{\delta z} + \eta\beta \qquad 6$$

where β is the regional value of the potential field and x_0, y_0, z_o defines the position of the source, which produce the total potential field T measured at (x, y, z), η is the structural index.

2.2.2.4 Tilt Derivative

A generalized definition for the local phase of a potential field function is known as the tilt derivative (or angle). Due to the efficient Automatic Gain Control (AGC) enforced by the arc tangent function, which restricts the tilt angle to within the range -90 to +90 independent of the amplitude or wavelength of the magnetic field, mapping the magnetic tilt angle offers the advantage of magnifying weak magnetic anomalies (Verduzco *et al.,* 2004).

Tilt derivative is used to estimate the location and depth of magnetic sources. It is based on a model of a buried 2D vertical contact and it is a very straightforward way to estimate the location and strike of geological contact/faults, as well as the depth to basement of magnetic anomalies (Fairhead *et al.,* 2009). Depths to a magnetic source are estimated by taking the average of the distance between +45^o and -45^o contour lines (Verduzco *et al.,* 2004; Salem *et al.,* 2007; Balogun, 2019). Tilt derivative is expressed mathematically as

Preprint not peer reviewed

This preprint research paper has not been peer reviewed. Electronic copy available at: https://ssrn.com/abstract=4072454

$$TDR = tan^{-1}\frac{VDR}{THD} \quad (7)$$

where VDR is the first vertical derivative and THD is the total horizontal derivative of the TMI respectively.

2.2.3 2D Electrical Resistivity Tomography (ERT) Data Processing

In order to process the 2D ERT data, Advance Geophysical Incorporated (AGI)'s "EarthImager software" was used to invert the data. Inversion of this kind is usually done by comparing the field measured data (model) with a corresponding theoretical model in order to generate an apparent resistivity inverted section (a solution) from the theoretical model that fits the measured field data. The difference between the field measured data and the corresponding theoretical model is expressed as the RMS error. The lower the RMS error, the higher the level of confidence in the result given by the inverted apparent resistivity pseudo-section generated.

2.2.4 Integration of Aeromagnetic and the 2D ERT Data

The Aeromagnetic and 2D ERT data were integrated so as to determine if lineaments delineated from aeromagnetic data can be confirmed from the 2D ERT results. If confirmed by both the results of the magnetic and electrical resistivity methods, a delineated lineament has thus been proved to exist within the subsurface beyond reasonable doubt.

3 Results and Discussion

3.1 The Total Magnetic Intensity (TMI) Field, Reduced to the Magnetic Equator (RTE) TMI and the Residual Magnetic Intensity Maps

3.1.1 The Total Magnetic Intensity (TMI) Field Map

The TMI map was observed to be dominated by elongated to linear magnetic anomalies trending mostly in the approximate N – S direction, with just a few trending in the approximate East – West direction (Figure 5). In general, the whole region showed four magnetic field intensity zones (Labeled A, B, C and D), which are characteristically distinct with magnetic intensity decreasing from West to East (Figure 5). Though, all the zones appear to be linear, they vary in shape and size. It should also be noted that magnetic relief across this whole region is rather low, being just 2.6 nT in value.

The study area (i.e. Mountain Top University's permanent site) lies predominantly within the highest (pink colouration) and intermediate (yellow and green) intensity zones (Figure 5). The

Preprint not peer reviewed

This preprint research paper has not been peer reviewed. Electronic copy available at: https://ssrn.com/abstract=4072454

pattern of the decreasing magnetic intensities eastwards seems to be suggestive of a step-faulting phenomenon with depth to the faulted block decreasing eastwards. It should also be noted that since the study area is located in a magnetic low latitude region, magnetic lows on the map represent bodies or structures having relatively higher magnetic susceptibility while the magnetic highs represent bodies or structures with relatively lower magnetic susceptibility.

3.1.2 Reduced to the Magnetic Equator (RTE) TMI Field

In an attempt to reduce some of the ambiguities that may be associated with magnetic data interpretation, especially the ambiguity due to magnetic inclination, the data was reduced to the

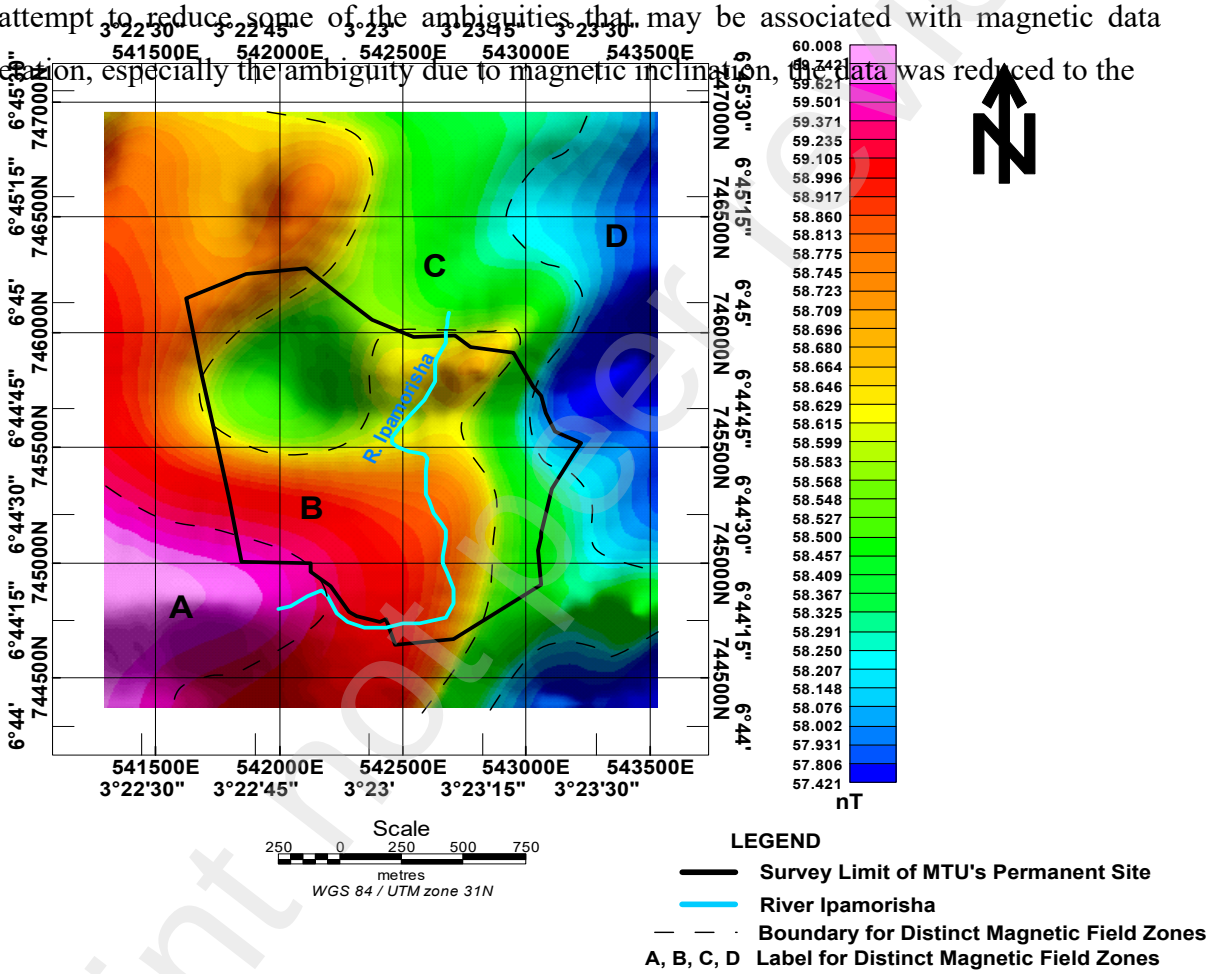

Figure 5: The Total Magnetic Intensity Field Map

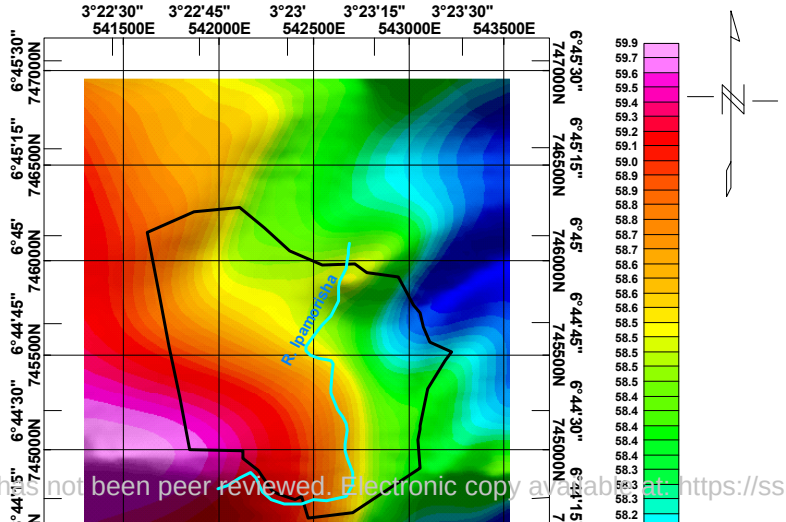

This preprint research paper has not been peer reviewed. Electronic copy available at: https://ssrn.com/abstract=4072454

Figure 6: The Reduced to the Magnetic Equator TMI Map

magnetic equator so that the resultant magnetic data can appear as if it were acquired at the magnetic equator. The advantage of this is that "magnetic inclination" asymmetry associated with anomalies can be removed and any form of enduring asymmetry can be considered as due to the attitude of the causative body.

Due to the fact the study area is close to the magnetic equator (magnetic inclination and declination at the place being -13.598^{o} and -1.669^{o} respectively), there was no significant observable difference between the TMI field map (Figure 5) and the RTE field map (Figure 6). The interpretation of both maps is essentially the same.

3.1.3 The Residual Field Map

First order regional field was removed from the RTE map to generate the first order residual field map (Figure 7). The residual field map was observered to comprise of both elongated and spherical magnetic anomalies, some with relatively high magnetic intensities while some have relative low magnetic intensities.

The northcentral to northeastern, southwestern and southeastern regions were dominated by elongated, relatively high magnetic field intensity anomalies. The northwestern part is made up of roughly spherical, relatively low magnetic intensity anomalies and the "central eastern" and southern parts are made-up of elongated but also relatively low magnetic anomalies. An intersection of magnetic lows (labeled "Y") in the eastern part of the study area suggests the possibility of the study area being a shear zone (Figure 7). When the TMI map (Figure 5) was compared with the residual map (Figure 7), it was found out that the residual map has accentuated the short wavelength structures and suppressed the long wavelength structures dominating the TMI

Preprint not peer reviewed

This preprint research paper has not been peer reviewed. Electronic copy available at: https://ssrn.com/abstract=4072454

map significantly. Figure 8 shows the first order regional field removed from the RTE in the process of generating the residual map.

3.2 Lineament Extraction

A combination of the Total Horizontal Derivative (THD), Euler Deconvolution and Tilt Derivative enhancement operations were employed for the delineation of geologic lineaments present in the study area. In geologic terms, these lineaments, where they are genuinely mapped usually indicate rock or lithologic contacts and fractures (i.e rock joints and faults).

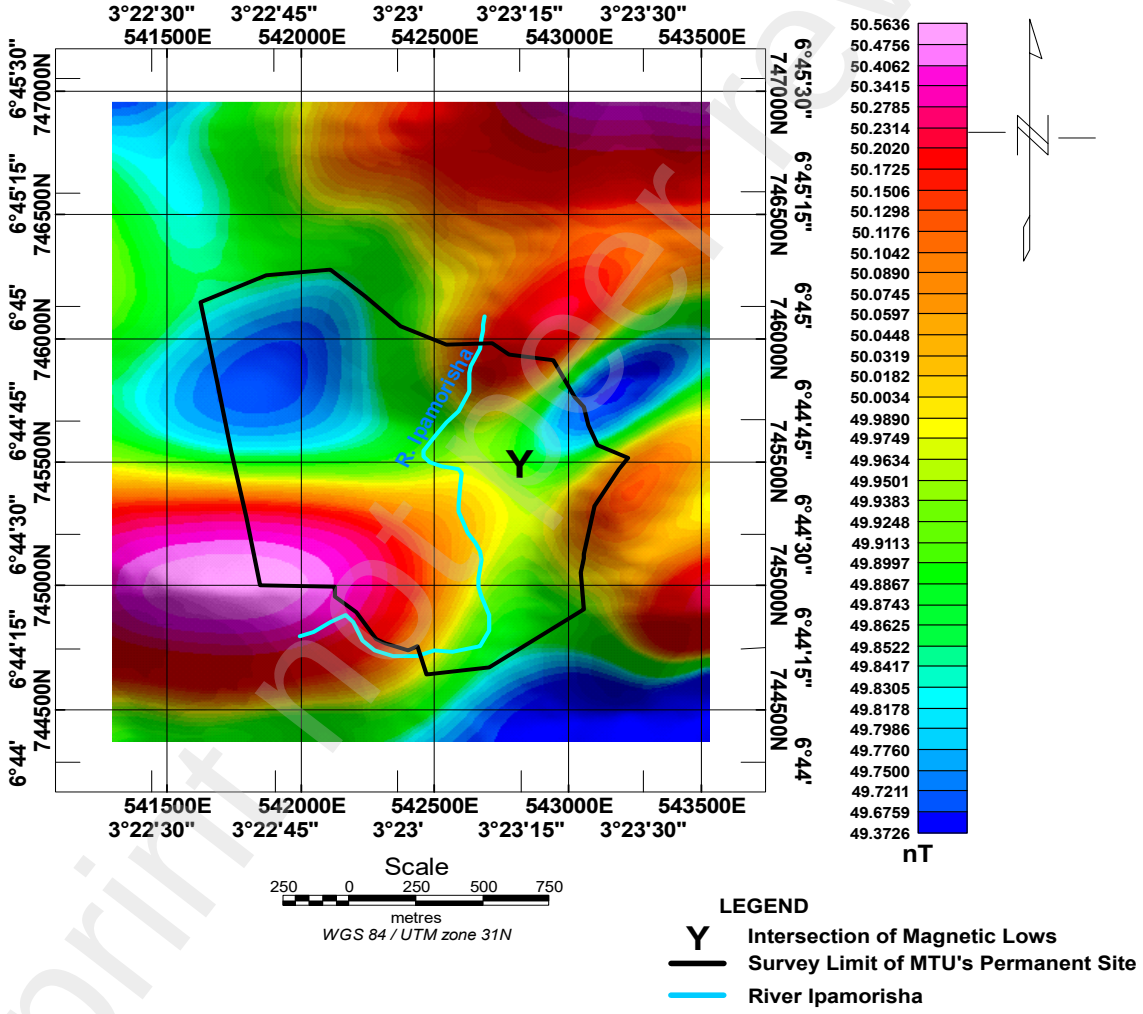

Figure 7: The Residual Field Map of the Study Area

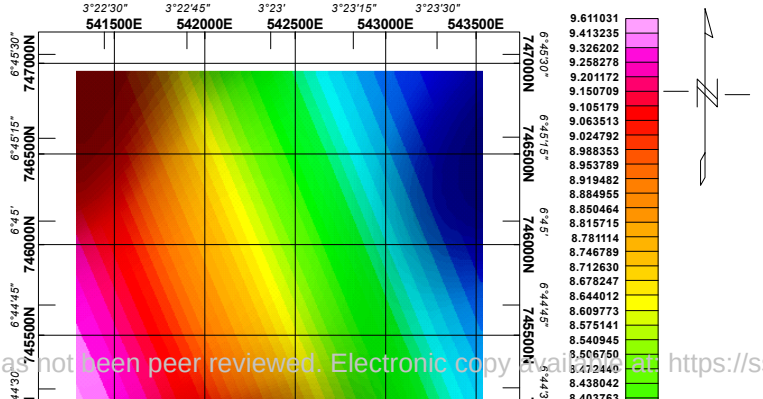

This preprint research paper has not been peer reviewed. Electronic copy available at: https://ssrn.com/abstract=4072454

Figure 8: The Regional Field Map of the Study Area

3.2.1 Total Horizontal Derivative

From the knowledge of the application of differential calculus, it can be established that the gradient of a function will be maximum at a region where there is an abrupt change or where discontinuity of the function is observed. In similar terms, we expect that when we perform the first order horizontal derivative of a potential field function such as gravity and magnetic field with respect to their areal extent, the regions of peak gradient (derivative) should indicate regions of discontinuity of such field and this in geological terms will be suggestive of linear geologic structures.

Total horizontal derivative was performed on the residual field data and fifteen (15) long to intermediate scaled lineaments (or curvilineaments) and several other local (short) scaled lineaments were delineated (Figures 9(a) and (b)).

A conspicuous wide zone of structural weakness (labeled A on Figure 9(a)), bounded to the West amd East by curvilineaments “2” and “3” respectively was delineated. The zone, covering most of the northwestern region where it has a width of 769.23 km, runs southwards, following the NW – SE trend initially before it changed course to continue due south and eventually terminating at the southeastern region where it thinned out to become only 128.2 m wide.

Five other zones of weakness, namely, B, C, D, E and F were observed at the eastern part of the study area. These zones are approximately parallel to one another and all trend in the approximate NE – SW direction. C, bounded by lineaments 4 and 5; D, bounded by lineaments 5 and 6; E,

Preprint not peer reviewed

This preprint research paper has not been peer reviewed. Electronic copy available at: https://ssrn.com/abstract=4072454

bounded by lineaments 6 and 7; and F, bounded by lineaments 7 and 8 all appear to terminate on curvilineament 3 and do not cut into Zone A. Only “Lineament 14”, bounding Zone B to the west, cuts into Zone A signifcantly.

From the cross-cutting relationship, three tectonic events can be established based on the imprints left behind. The oldest is a first NE-SW trending event that formed the zones of weakness C, D, E and F. The second is the approximate NW-SE event that brought about the zone of weakness A which cut through structures C, D, E and F. The last observable event is also a NE-SW trending event, significantly represented by “Lineament 14” that cuts through Zone A at the northwestern end of the permanent site (Figure 9 (a)). It is most likely the youngest of all the events. The severe deformation observed in the study area presents the study area as a shear zone.

3.2.1.1 The broad semi-elliptical peak at the south-western corner of the THD map

A broad semi-elliptical peak bounded by “curvilineament 2” and on which “curvilineament 1” is centred was observed at the south-western corner of the THD map (Figure 9(a)). Based on its location, this peak, broad signature is suggested as the THD response of the elliptical magnetic-high anomaly located at the south-western region of the residual field map (Figure 7). Due to the anomaly shape and appearance, the causative body is likely to be an elliptical cone (Figure 7) in terms of shape. The anomaly is predicted to be likely an accumulation of superficial (sand) deposits within and around the old channels of river Ogun which had abandoned at least one course within the vicinity.

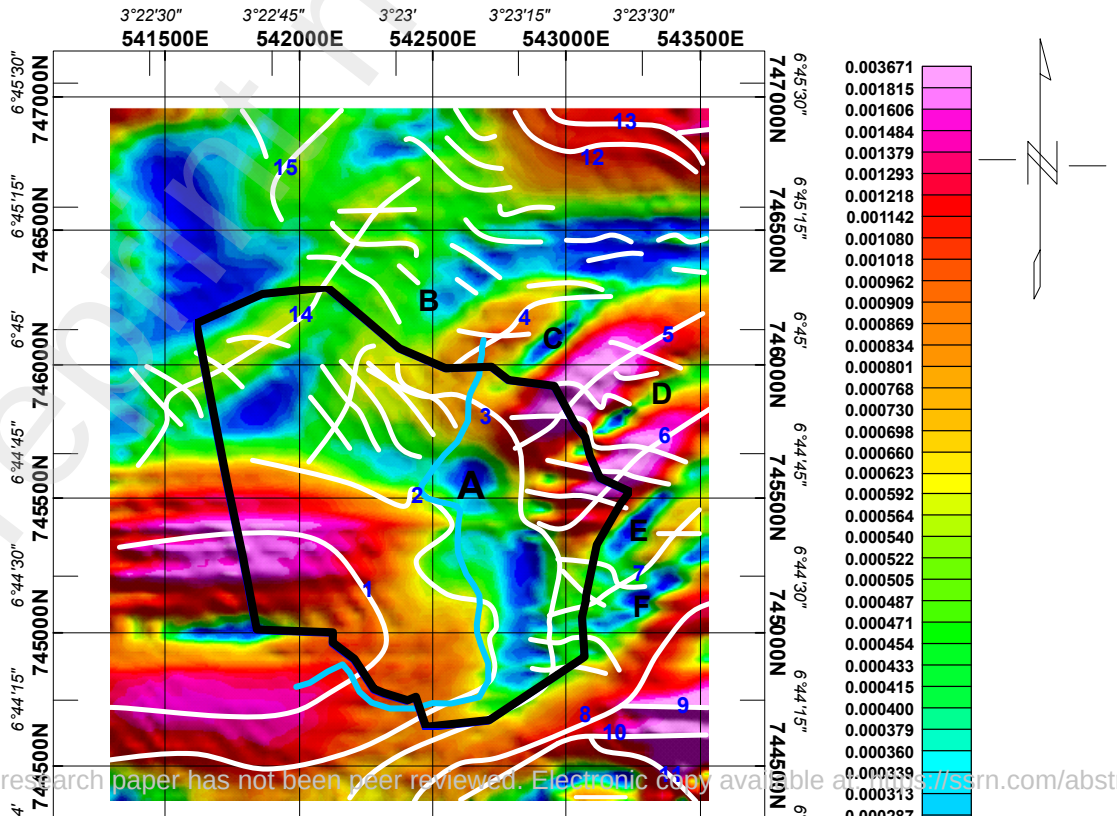

This preprint research paper has not been peer reviewed. Electronic copy available at: https://ssrn.com/abstract=4072454

Figure 9(a): The Total Horizontal Derivative Map of the Study Area

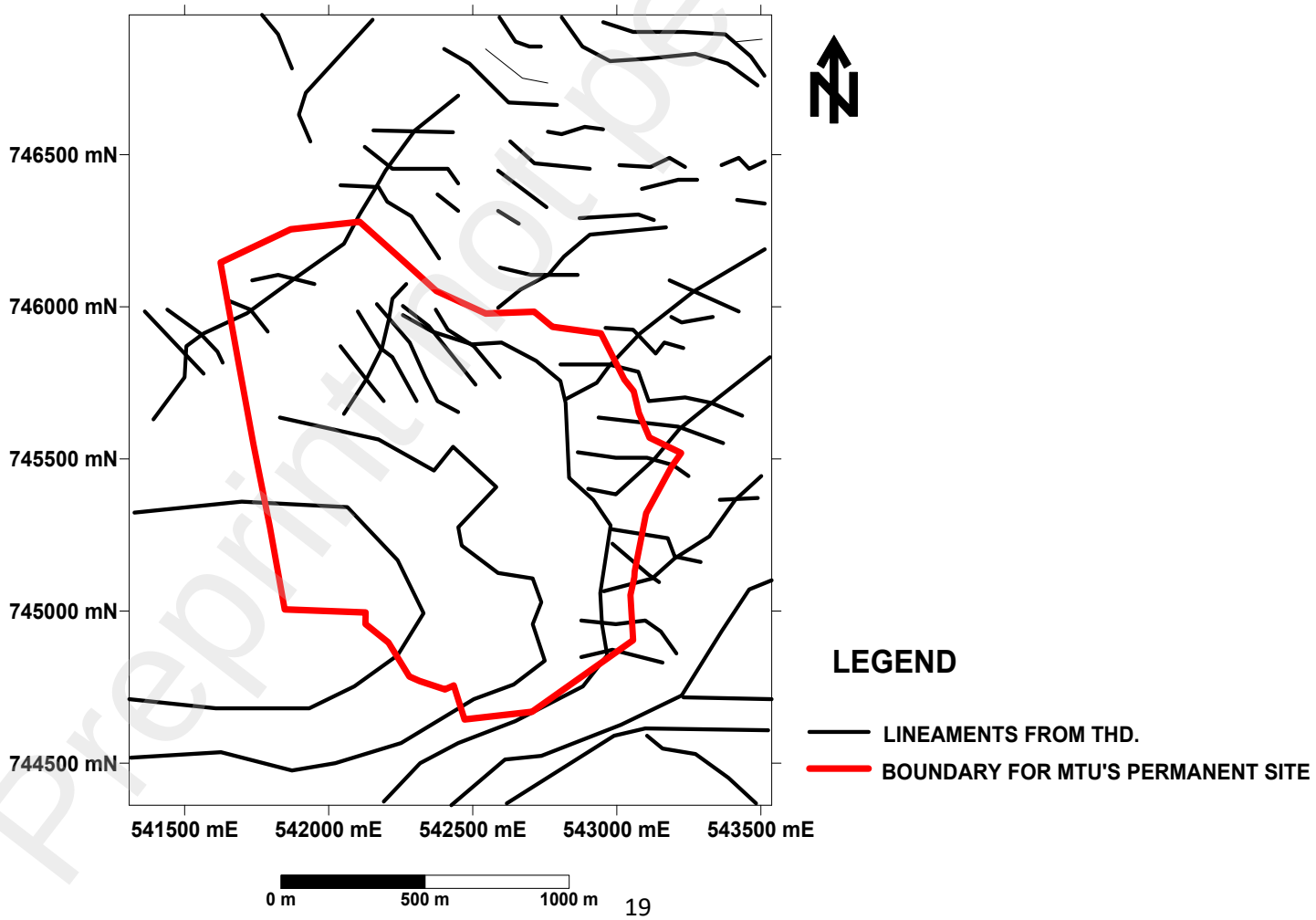

Preprint not peer reviewed

This preprint research paper has not been peer reviewed. Electronic copy available at: https://ssrn.com/abstract=4072454

Figure 9(b): The Lineaments Delineated from Total Horizontal Derivative Operation

3.2.2 Euler Deconvolution

Euler deconvolution solutions for the data were obtained using the Euler's homogeneity equation presented in equation 6 and the solutions were plotted as color ranged symbols in Figure 10. Since the scope of the work is to delineate linear geologic strucures, a structural index of zero, representing the model for linear geologic structures, was adopted for generating the solutions. It was discovered that only the long and intermediate ranged lineaments were well resolved by the Euler Deconvolution solution plot (Figures 10(a) and 10(b)). The plot presents most of the lineaments to have depths that rarely exceeds 200 m except at some few locations.

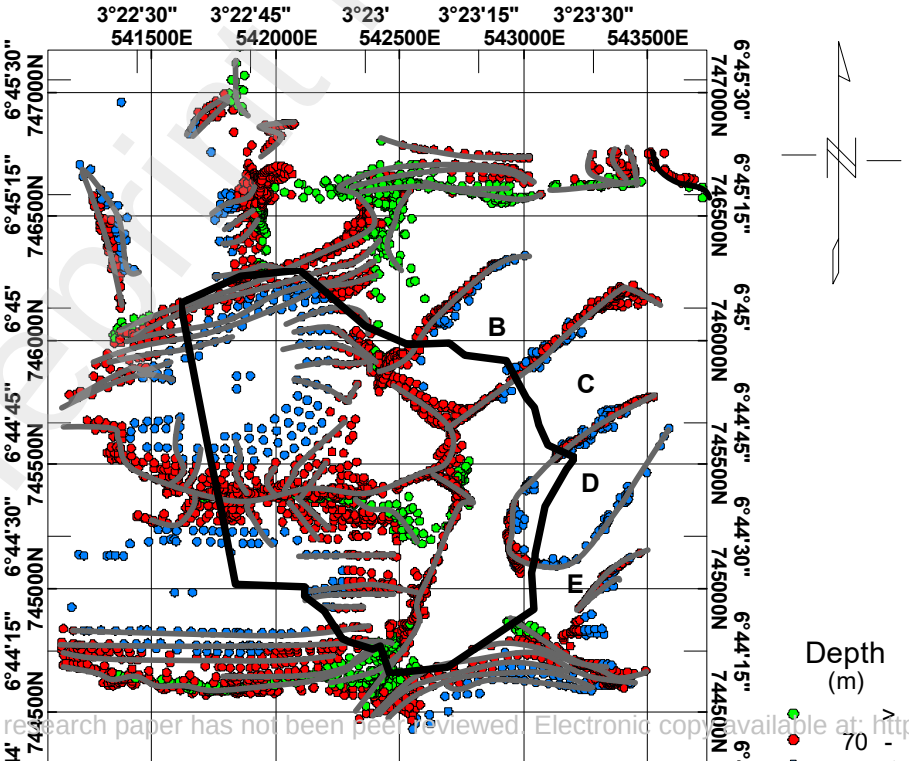

This preprint research paper has not been peer reviewed. Electronic copy available at: https://ssrn.com/abstract=4072454

Figure 10(a): The Euler Deconvolution Solution Plot of the Study Area

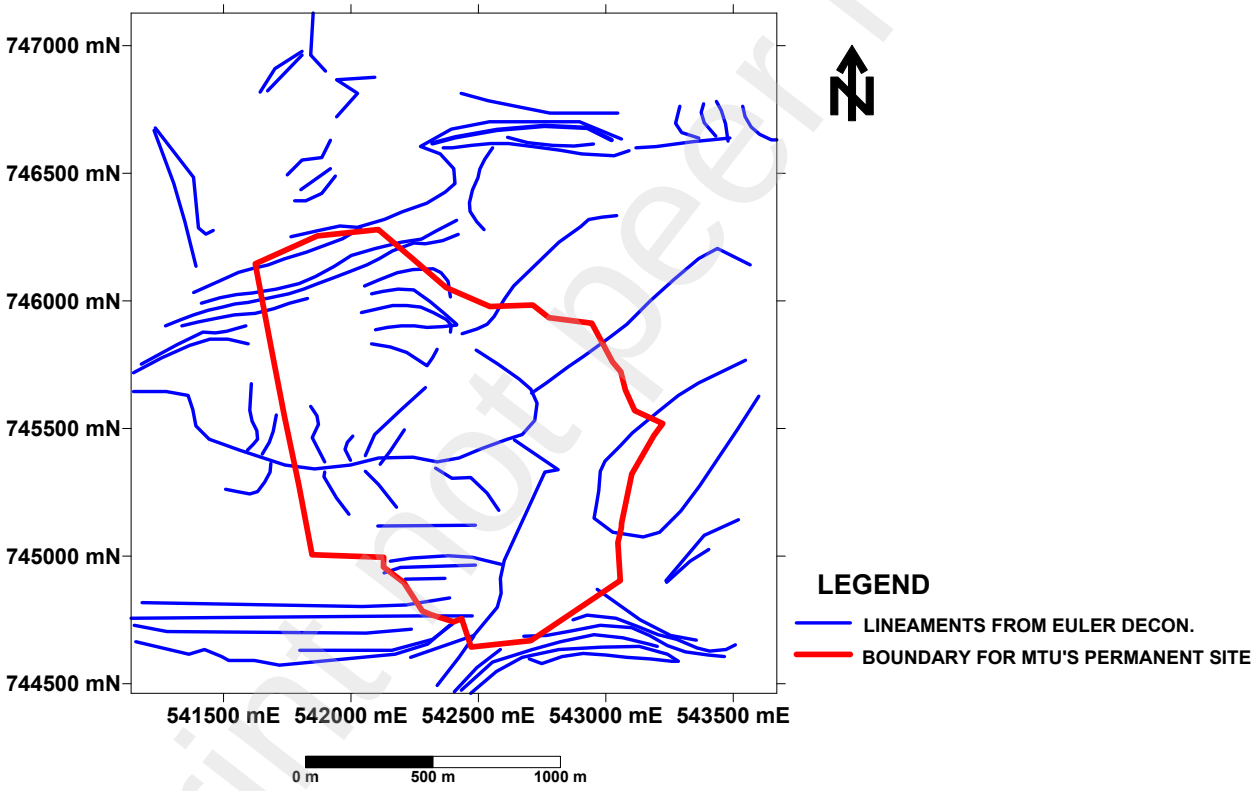

Figure 10(b): The Lineaments Delineated from Total Euler Deconvolution Solution Plot

3.2.3 Tilt Derivative (TDR)

In the interpretation of tilt derivative solutions (map), 0^{o} lines are taken to represent regions of discontinuities (lineaments). The tilt derivative solutions delineated three major lineaments (Figure 11 (a) and (b)). The lineaments delineated by tilt derivative are regional in nature and it sufficiently

Preprint not peer reviewed

This preprint research paper has not been peer reviewed. Electronic copy available at: https://ssrn.com/abstract=4072454

outlined the edges of the intersecting magnetic lows designated “Y” on the residual field map presented in Figure 7. The “Y” region are presented as a zone of weakness.`

3.2.4 Integration of the Extracted Lineaments from the aeromagnetic data using the Various Enhancement Techniques

The lineaments delineated by the THD comprised of long, intermediate and short lineaments. The western and southern parts consist mostly of long and intermediate lineaments while the northeastern part is dominated by short lineaments (Figure 9(b)). The Euler Deconvolution mostly resolved long lineaments and their appendages but resolved less of isolated short lineaments (Figure 10(b)). The integrated result of the THD and Euler deconvolution derived lineaments appeared to be confirmatory in most parts (i.e. the results agreed) while in some parts it was complementary as they seemed to complement each other (Figure 12(a)).

In order to reduce overclustering of the lineaments as was observed in Figure 12(a), lineaments greater than 200 m for the THD, Euler deconvolution and TDR were presented in Figure 12(b). The lineaments have orientations ranging from N-S, E-W, NW-SE and NE-SW though the dominant orientations are the E-W and the NW-SE orientations (Figure 13).

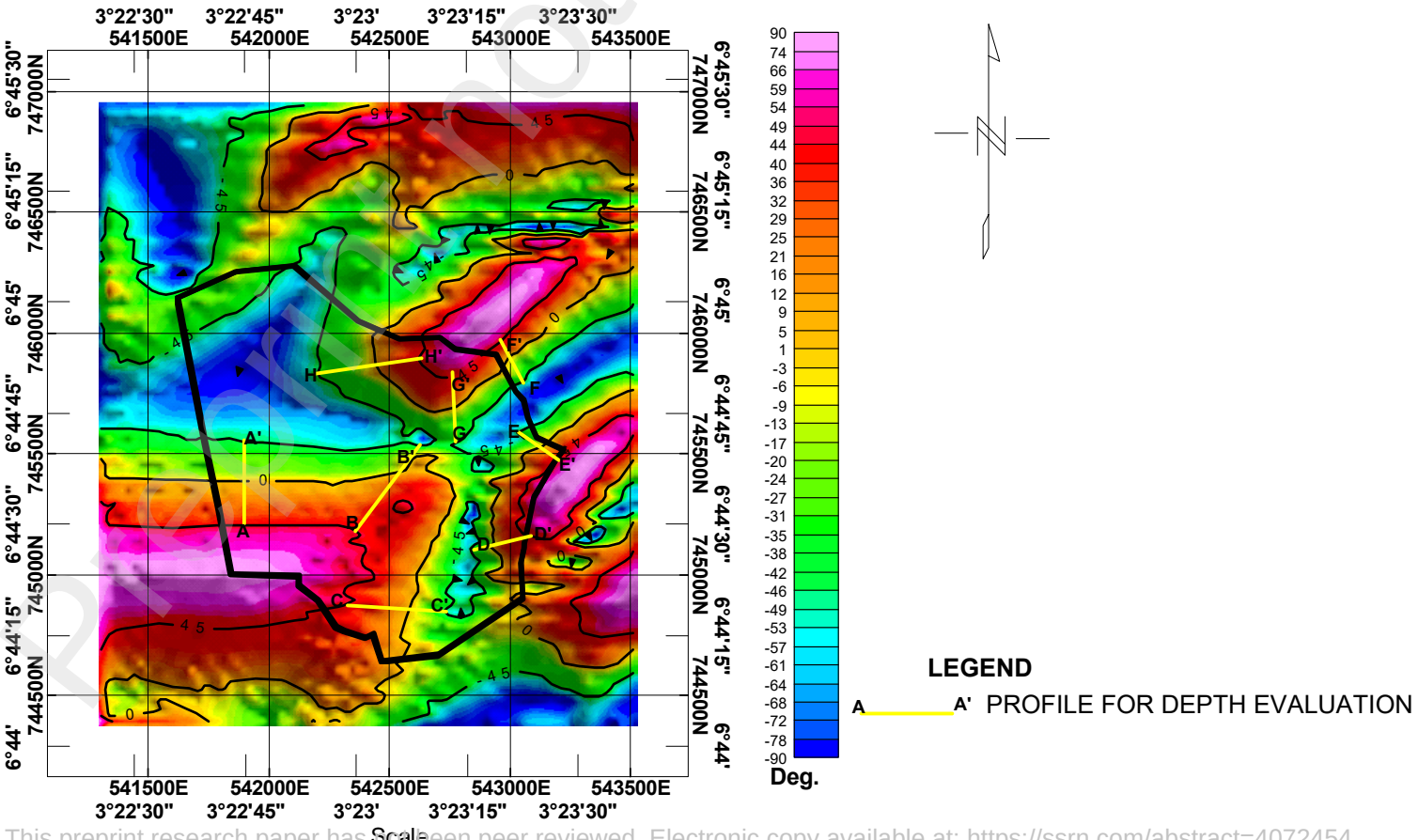

This preprint research paper has not been peer reviewed. Electronic copy available at: https://ssrn.com/abstract=4072454

Figure 11(a): The Tilt Derivative Map of the Study Area

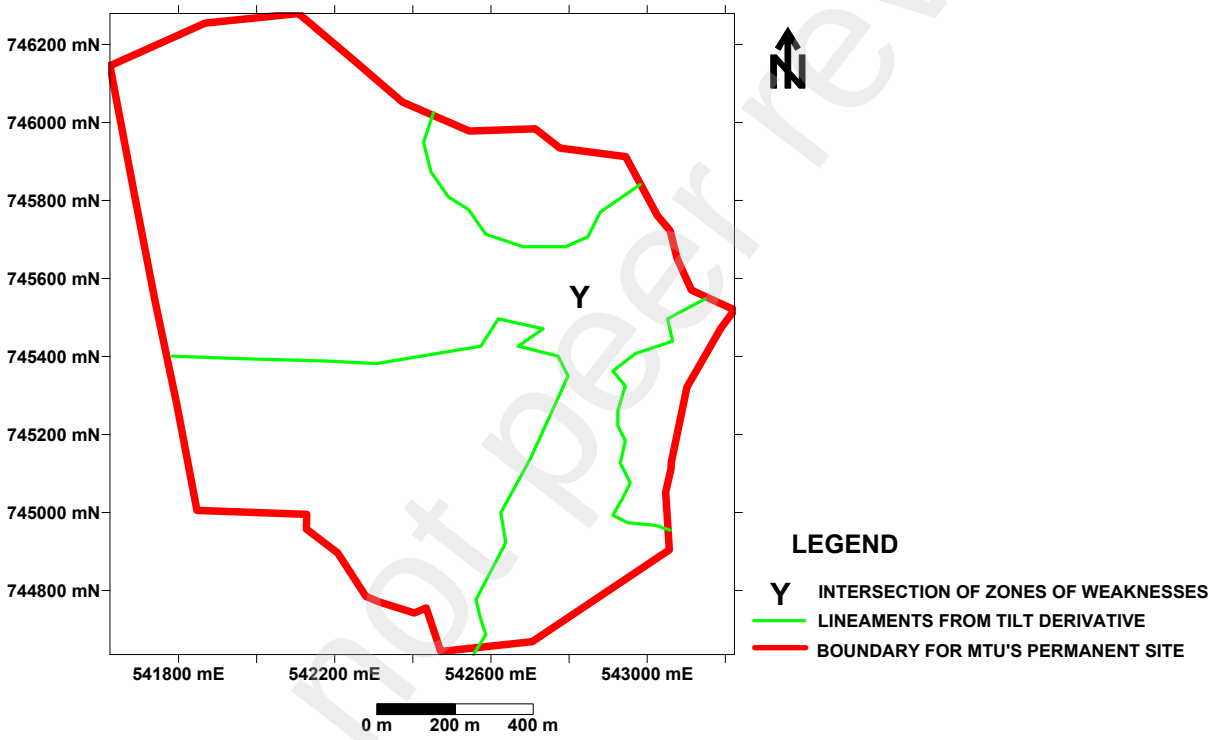

Figure 11(b): The Lineaments Derived from the Tilt Derivative Map of the Study Area

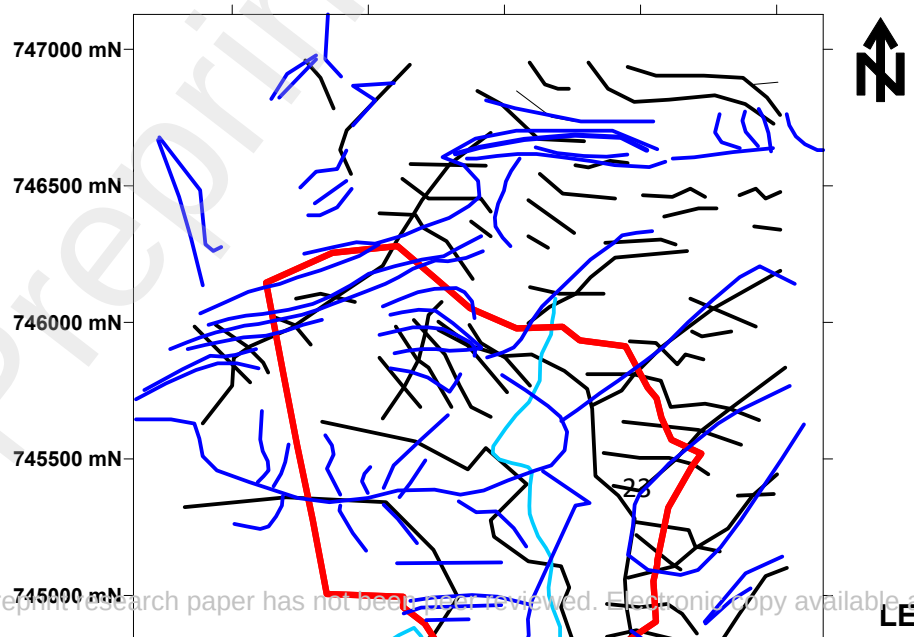

Preprint not peer reviewed

This preprint research paper has not been peer reviewed. Electronic copy available at: https://ssrn.com/abstract=4072454

Figure 12(a): Integrated Lineaments Derived from the THD and Euler Deconvolution Operations

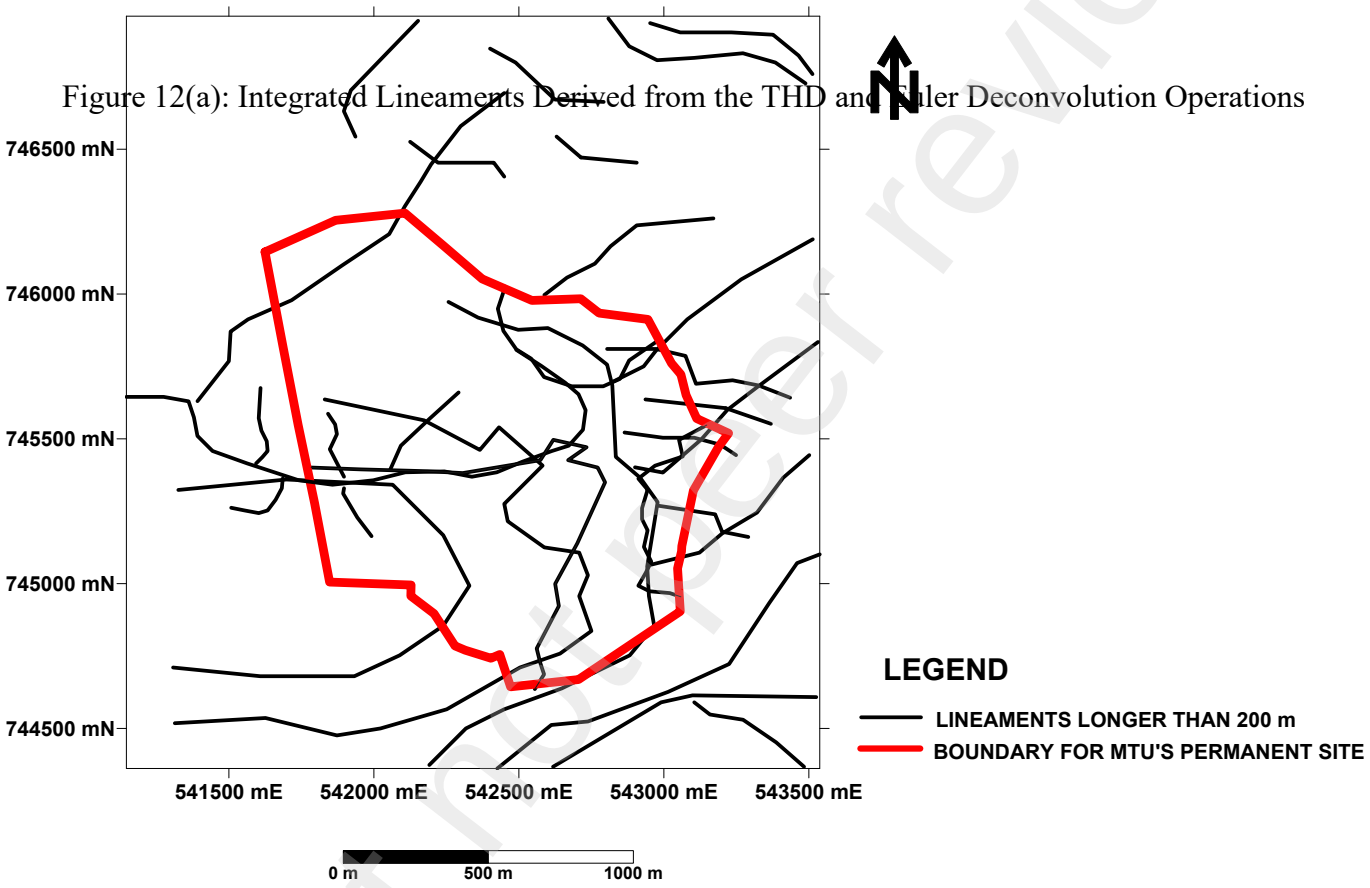

Figure 12(b): Lineaments Longer than 200 m Derived from the Combination of THD, Euler Deconvolution and Tilt Derivative Operations

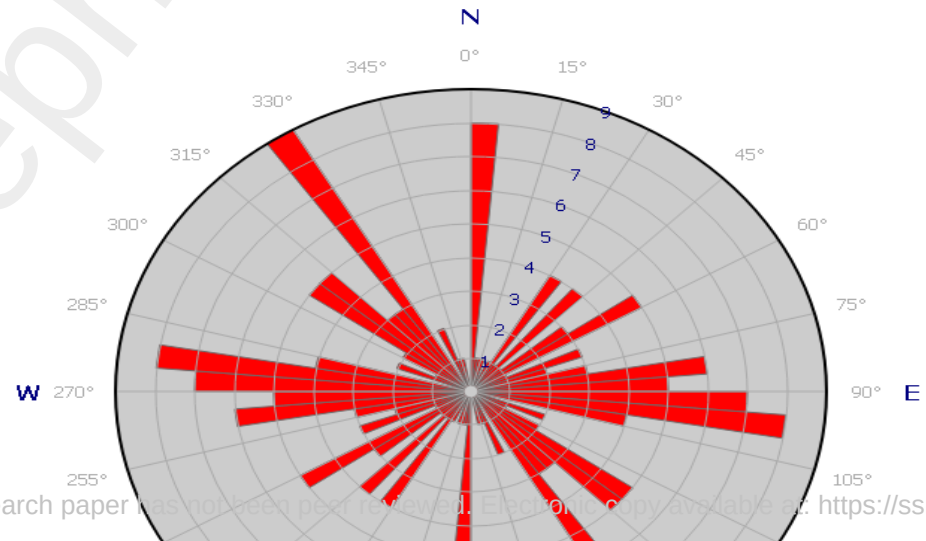

Preprint not peer reviewed

This preprint research paper has not been peer reviewed. Electronic copy available at: https://ssrn.com/abstract=4072454

Figure 13: Rose Diagram Showing the Orientations of the Magnetic Lineaments Delineated.

3.2.5 Comparison of Depth Estimates from Euler Deconvolution and Tilt Derivative

Based on the Euler deconvolution map, the depth of lineaments delineated rarely exceeded 200 m except in the central southern and central northern parts where parts of a few lineament were found to be deeper (Figure 10(a)). To estimate depths to delineated lineaments (usually located on 0^o contour lines) on the tilt derivative map, distance between $+45^o$ and -45^o contour lines are determined and depth to the 0^o contour line (indicating locations of linear geologic structures) located between the $+45^o$ and -45^o contour lines, are computed as half the distance obtained between $+45^o$ and -45^o contour lines, using the scale of the map.

To determine depths to the southwestern structure on the tilt derivative map, Profiles A-A', B-B' and C-C' were taken over the structure and the depths obtained were 176.44 m, 235.29 m and 286.76 m respectively. To determine depths to the eastern structure, Profiles D-D' and E-E' were taken over it and the depths obtained were 132.35 m and 110.29 m respectively. To determine the depths to the northeastern structure, Profiles F-F', G-G' and H-H' were taken over it and the depths obtained were 102.94 m, 147.06 m and 220.59 m respectively.

Intepreted in terms of dip, the northeastern structure dips towards the west within the study area, while the southwestern and eastern stuctures both dip towards the south.

3.3 The 2D Electrical Resisitivity Tomography (ERT) Data Interpretation

Four 2D ERT data, labelled 2D ERT Line 1, 2D ERT Line 2, 2D ERT Line 3 and 2D ERT Line 5, were acquired within the study area. The four profiles were 1110 m long and probed up to a depth of 220 m. When superimposed on the delineated magnetic lineaments (Figure 14), the 2D ERT profiles were found to cut across some of the lineaments.

Preprint not peer reviewed

This preprint research paper has not been peer reviewed. Electronic copy available at: https://ssrn.com/abstract=4072454

3.3.1 2D ERT Line 1 (Figure 15(a))

As observed on Figure 14, "2D ERT Line 1" was noted to cut across 7 magnetic lineaments which are located at 117 m, 208 m, 243 m, 299 m, 425 m, 741 m and 891 m from the start of profile. Only the lineaments located at 117 m (110 m on 2D ERT profile), 208 m to 243 m (200 to 250 m on 2D ERT profile), 425 m (440 m on 2D ERT profile) and 891 m from the start of profile were visble on the 2D ERT section. Point 741 from the start of line only showed as a "kink", designated as K, on the 2D ERT section (Figure 15(a)). To a good approximation, three basic

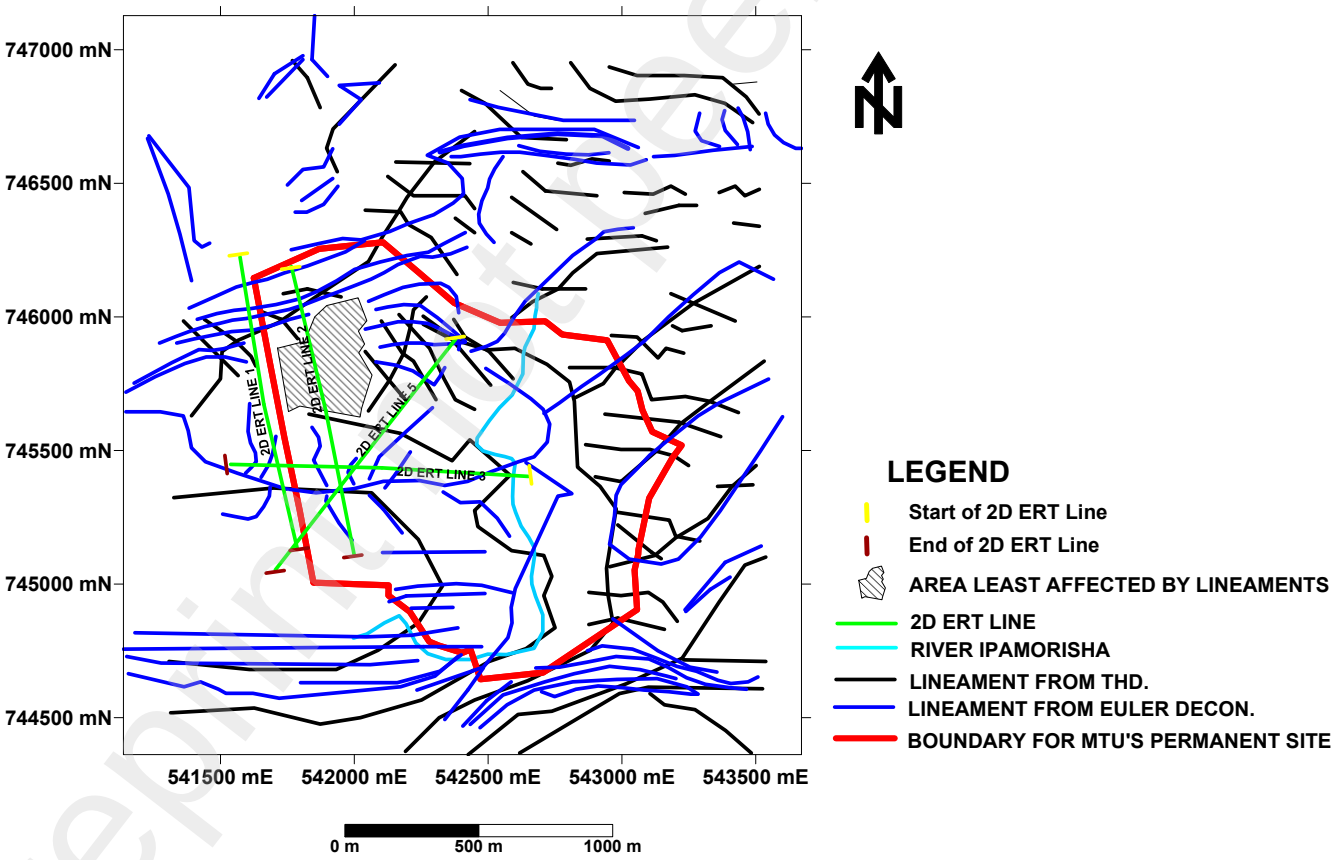

Preprint not peer reviewed

This preprint research paper has not been peer reviewed. Electronic copy available at: https://ssrn.com/abstract=4072454

Figure 14: Map Showing the Positions of the 2D ERT Profiles Relative to the Delineated Magnetic Lineaments

Preprint not peer reviewed

This preprint research paper has not been peer reviewed. Electronic copy available at: https://ssrn.com/abstract=4072454

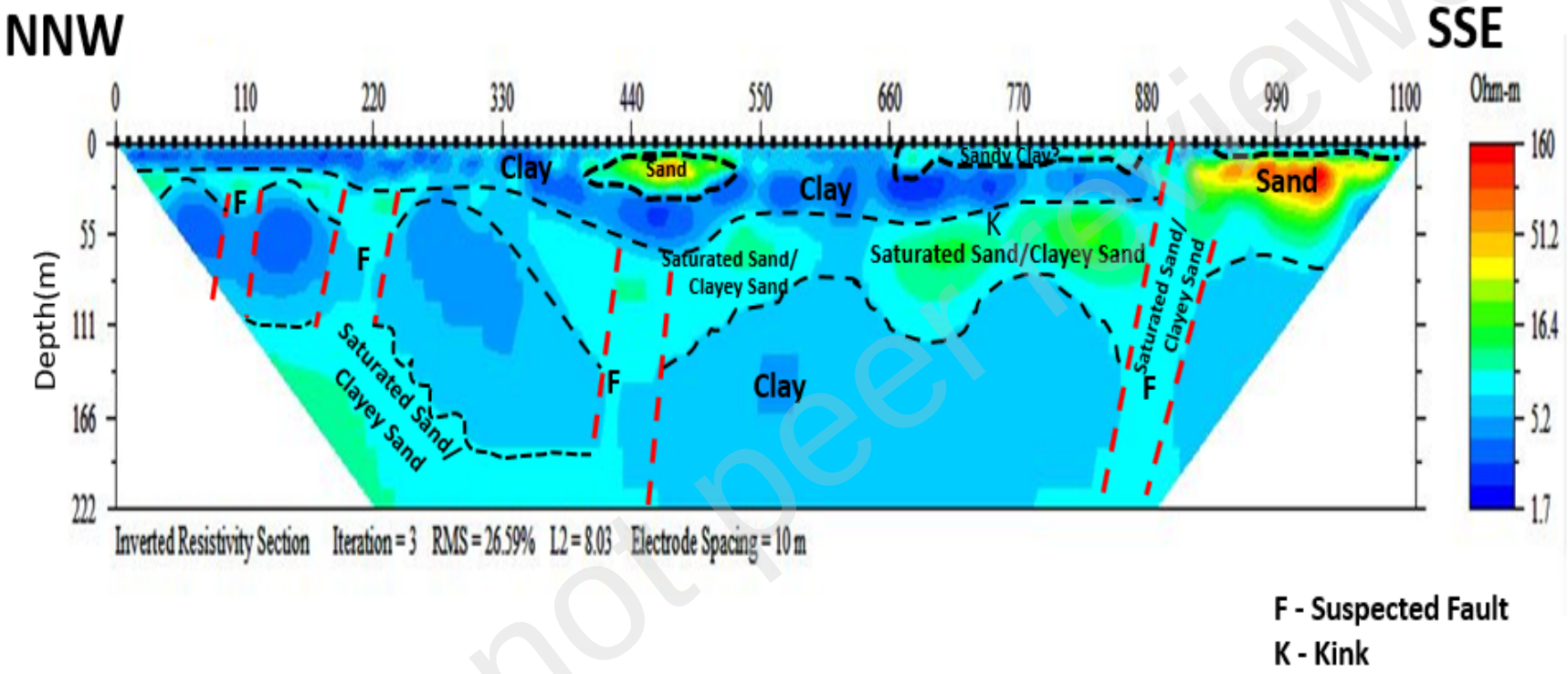

Figure 15(a): 2D ERT Line 1

Preprint not peer reviewed

This preprint research paper has not been peer reviewed. Electronic copy available at: https://ssrn.com/abstract=4072454

lithologies (which are clay, sand and saturated sand/clayey sand) constituting four geoelectric/geologic layers which include a "clay" first layer, a "saturated sand/clayey-sand" second layer, a "clay" third layer and a "saturated sand/clayey sand" fourth layer were delineated in the northern section. In the central part (400 m to 530 m), a pocket of sand was delineated to be embeded within the first layer which is clay. At the southern end, three geoelectric layers which include a topmost thin layer of clay, followed by a considerably thick layer of sand (about 70 m) extending from a depth of about 8 m to 77.5 m, and last layer which is clayey in nature.

3.3.2 2D ERT Line 2 (Figure 15(b))

This profile is located 230 m east of "2D ERT Line 1". As can be seen on Figure 14, "2D ERT Line 2" cuts across 8 magnetic lineaments which were located at 22 m, 99 m, 131 m, 161 m, 196 m, 589 m, 870 m and 1050 m from the start of profile. At about 195 to 225 m from the start of the profile is a region between two kinks, K_1 and K_2, conciding with the begining of a conspicous fault region which has been filled with sand (Figure 15(b)). K_1 is suspected to be the magnetic lineament intersected by the 2D ERT at 196 m from the start of profile. Points 870 to 890 m and 940 m to 990 m away from the start of the profile also appeared on the 2D ERT as "fault regions" and this also agreed in part with the result of the magnetic method that delineated a lineament at 870 m from the start of 2D ERT Line 2. The magnetic data seemed to be very responsive to edges formed by deposited superficial aggregate of earth materials (sand) as some magnetic lineaments (131 m, 161 m, 589 m and 1050 m) were found to be coincident with edges of gentle to signifcantly undulating layer of sand (undulating thickness of sand strata). A suspected ancient river channel was imaged at point 410 m from the start of line on the 2D ERT section. Just as was observed along profile 2D ERT Line 2, three basic lithologies which were "clay", "sand" and "saturated sand/clayey-sand" were delineated.

3.3.3 2D ERT Line 3 (Figure 15(c))

As observed on Figure 14, "2D ERT Line 3" was noted to cut across 7 magnetic lineaments which were located at 82 m, 170 m, 494 m, 681 m, 802 m, 981 m and 1037 m from the start of profile. Only the magnetic lineaments located at 981 m and 1037 m from the start of the 2D ERT Profile (2D ERT Profile 3), were consipicously imaged on the 2D ERT section. The lineament located at 981 m from the start of line was imaged as a prominent edge (labelled K on the ERT section) on a sand deposit at the eastern end and the lineament located at 1037 m from the start of the profile concides with a depression (labelled F?) on the ERT section. The lithologies delineated here were basically sand and clay.

Preprint not peer reviewed

This preprint research paper has not been peer reviewed. Electronic copy available at: https://ssrn.com/abstract=4072454

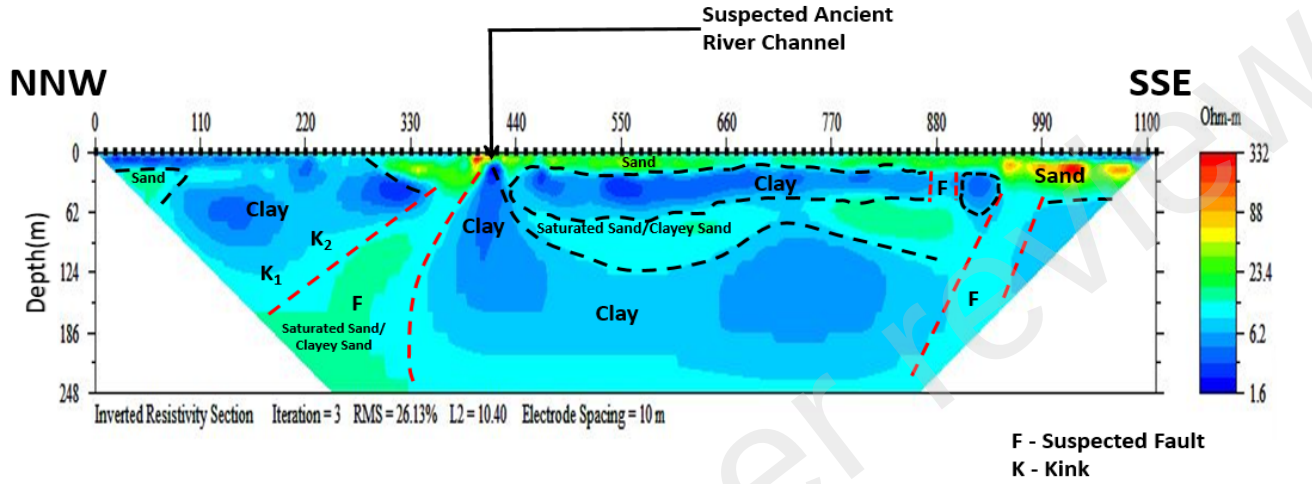

Figure 15(b): 2D ERT Line 2

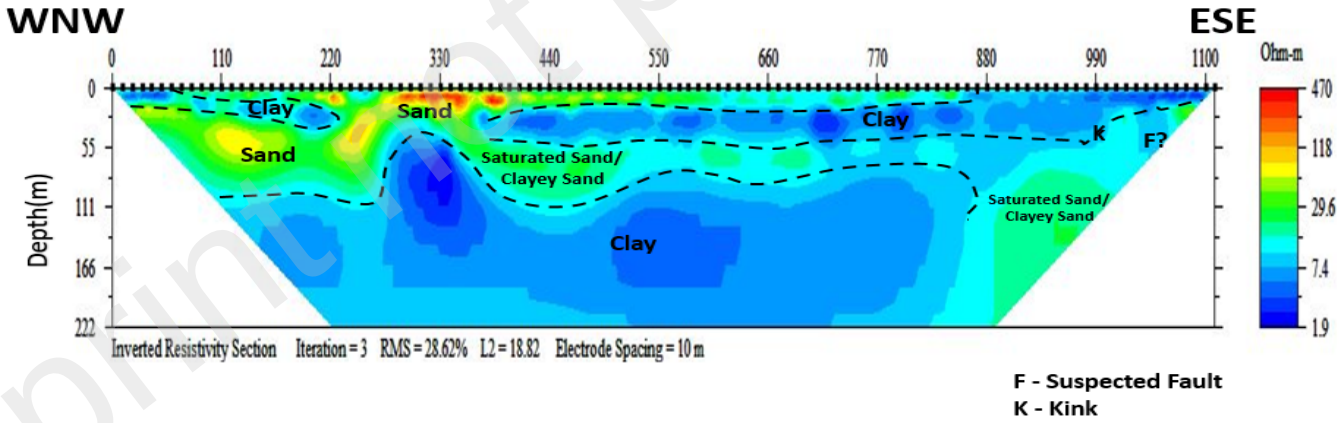

Figure 15(c): 2D ERT Line 3

Preprint not peer reviewed

This preprint research paper has not been peer reviewed. Electronic copy available at: https://ssrn.com/abstract=4072454

3.3.4 2D ERT Line 5 (Figure 15(d))

As observed on Figure 14, "2D ERT Line 5" is a NE-SW trending profile cuting across 7 magnetic lineaments which are located at 0 m, 26 m, 118 m, 192 m, 437 m, 656 m and 787 m from the start of profile. Points 192 m, 437 m and 656 m (610 – 640 m on the 2D ERT section) concide with suspected fault zones. Lithologies delineated are basically intercallation of sand and clay.

3.4 Implications of the Findings on the Physical Development of Mountain Top University's Permanent Site

Interpretation of the residual field and the lineament maps showed that the study area (Mountain Top University's permanent site) is a shear zone littered with lots of lineaments (Figures 7, 12(a) and 12(b)). The lineaments delineated have varying lengths. Depths of delineated lineaments rarely exceeded 287 m. In terms of lineament density, the least affected portion is a portion in the northwestern region identified as "area least affected by lineaments" (Figure 14). The implication of this is that the property must be developed with caution. The lineaments must be studied to determine if they are active or not before any form of construction. Special foundations may be required for construction. If faulted regions can be effectively stabilised for engineering constructions, the identified least affected portion by lineaments can then be used for landfill construction/waste management. As observed from the 2D ERT sections, the immediate topsoil at a considerable part of the study area is clay or clayey with thickness approching 8 m in some areas (e.g. northern to central part of 2D ERT Line 1, northern end of 2D ERT Line 2, eastern end of 2D ERT Line 3 and southwestern end of 2D ERT Line 5). This implies that the subgrade soil may be plastic and incompetent to carry heavy engineering structures. Other than stabilisng the faults if found to be inactive, it is also necessary to restrict constructions to regions where the subgrade soil is sandy and have appreciable thickness (exceeding 5 m). Search for groundwater may be concentrated around mapped faults, especially the ones identified on the 2D ERT sections. Based on their appearance and resistivity values on the 2D ERT sections, the delineated faults are suspected to be filled with sand.

Preprint not peer reviewed

This preprint research paper has not been peer reviewed. Electronic copy available at: https://ssrn.com/abstract=4072454

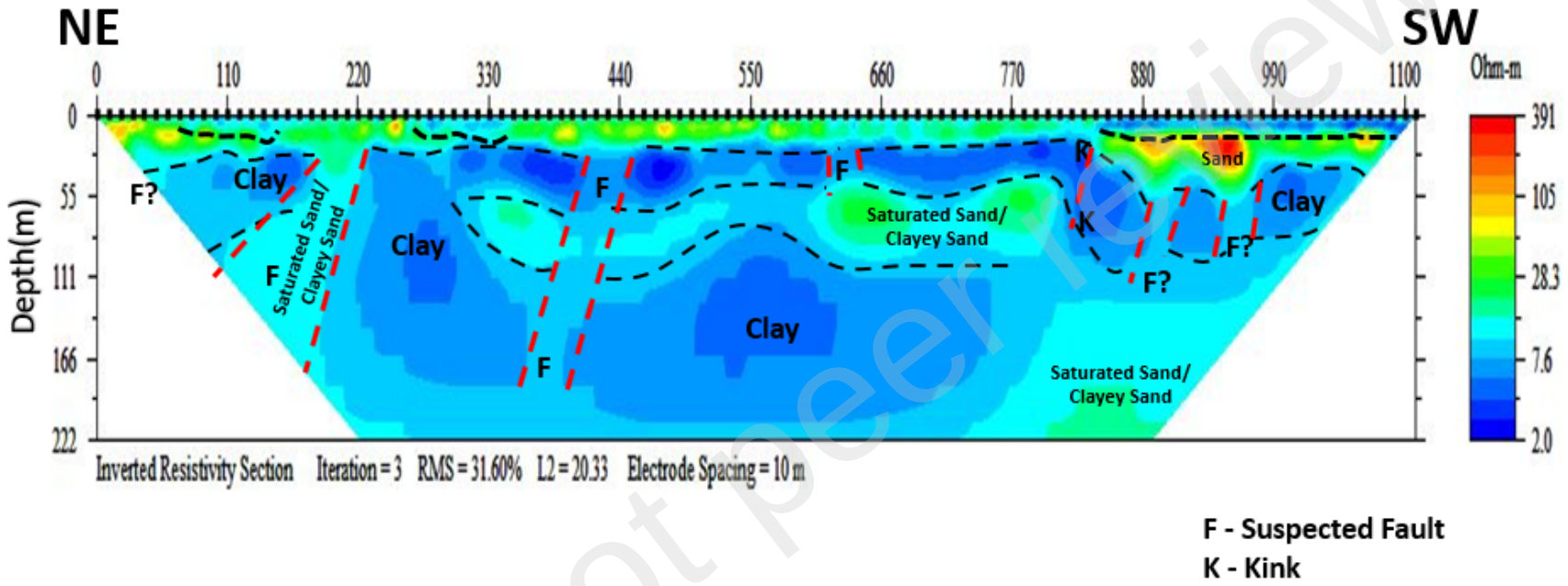

Figure 15(d): 2D ERT Line 5

Preprint not peer reviewed

This preprint research paper has not been peer reviewed. Electronic copy available at: https://ssrn.com/abstract=4072454

4 Conclusion

The study area was found to be a shear zone having lots of linear geologic structures within it. At least three tectonic events were established based on their imprints. The oldest was a first NE-SW trending event, the second was the approximate NW-SE event and the last observable event was another NE-SW trending event which appeared to be the youngest of all the events.

From the four 2D ERT data which were acquired to cut across delineated magnetic lineaments, some of the delineated magnetic lineament were confiremed on the 2D ERT sections to be genuine geologic faults while others only corresponded to edges along delineated strata of sand layer. The lithologies delineated were basically sand and clay. Euler Deconvolution solutions showed that depth estimates of linear geologic structures rarely exceed 200 m in the study area except in the central southern and central northern parts. Tilt derivative solutions present depth to some delineated semi-regional to regional scaled structures to range between 102.94 m and 286.76 m.

With respect to developmental planning, since lineament density seems to be high, the study area must be developed with caution. The lineaments must be studied to determine if they are active or not before any form of construction. The immediate topsoil at a good part of the study area is clayey, with thickness approaching 8 m in some areas. This implies that the subgrade soil may be plastic and incompetent to carry heavy engineering structures. Other than stabilisng the faults if found to be inactive, it is also necessary to restrict constructions to regions where the subgrade soil is sandy and have appreciable thickness (exceeding 5 m). Groundwater exploration should be concentrated around mapped faults, especially the ones identified on the 2D ERT sections. To optimize the groundwater resources in the area, the linear geologic structures which were all observed to dip towards the north on the 2D ERT profiles should be intersected at their direction of dip.

Preprint not peer reviewed

This preprint research paper has not been peer reviewed. Electronic copy available at: https://ssrn.com/abstract=4072454

REFERENCE

Adagunodo, T.A., Sunmonu, L.A. and Adetunji, A.A. (2015). An Overview of Magnetic Method in Mineral Exploration. Journal of Ecology and Environment 3(1), pp. 13-28

Adamo, N., Al-Ansari, N., Sissakian, V., Laue, J. and Knutsson, S. (2021). Geophysical Methods and their Applications in Dam Safety Monitoring. Journal of Earth Sciences and Geotechnical Engineering, 11(1), 291-345.

Adeleke, B. O. and Leong, G. C. (1978). Certificate Physical and Human Geography, West African Ed. Oxford University Press, Nigeria, Ibadan. pp. 32.

Balogun, O. B. (2019). Tectonic and structural analysis of the Migmatite–Gneiss–Quartzite complex of Ilorin area from aeromagnetic data. NRIAG Journal of Astronomy and geophysics, 8(1), 22-33.

Balogun, O.B, Ojo, S.B and Olorunfemi, M.O (2016). Characterisation of the tectonic lineaments in the central equatorial Atlantic region of Africa from Bouger anomaly gravity data. Ife Journal of Science 18(4); 931-947.

Bogoslovsky, V. A., and Ogilvy, A. A. (1977). Geophysical methods for the investigation of landslides. Geophysics, 42(3), 562-571.

Cardarelli, E., Cercato, M., Cerreto, A. and Di Filippo, G., 2010. Electrical resistivity and seismic refraction tomography to detect buried cavities. *Geophysical prospecting*, *58*(4), pp.685-695.

Curtis, C. and Low, N. (2016). Institutional barriers to sustainable transport. Routledge, pp.

Davis, K., Li, Y. and Batzle, M. (2008). Time-lapse gravity monitoring: A systematic 4D approach with application to aquifer storage and recovery. Geophysics, 73(6), WA61-WA69.

De Klasz, I., and Du Chêne, R. J. (1978). Presence of Albian-Cenomanian in southwestern Nigeria and its paleogeographic implications. Compte Rendu de la Société de Physique et d'Histoire Naturelle de Genève, 13, 10-15.

Dearman, W. R. (2013). Engineering geological mapping. Elsevier.

Delury, D.B (1950). Values and Integrals of the orthogonal polinomials up to n = 26. University of Toronto press.

Preprint not peer reviewed

This preprint research paper has not been peer reviewed. Electronic copy available at: https://ssrn.com/abstract=4072454

Fairbridge, R.W., Askew, A.J., Herschy, R.W., Herschy, R.W., Herschy, R.W., Hordon, R.M., Muller, R.A., Grymes, J.M., Fairbridge, R.W., Herschy, R.W. and Brassington, F.C., 1998. Water movement in unsaturated soils. *Encyclopedia of Hydrology and Water Resources*, pp.699-706.

Fairhead, J. D., Salem, A., and Williams, S. E. (2009). PS Tilt-Depth: A Simple Depth-Estimation Method Using First Order Magnetic Derivatives.

Google Maps (2020), Mountain Top University Permanent Site, Makogi-Oba, Ogun State, Nigeria, 1: 1500. Google Maps Online, Accessed August, 2021.

Gore, D. and Davies, P. (2013). Background paper on produced water and solids in relation to coal seam gas production.

Grant, F.S (1957). A problem in the analysis of geophysical data. Geophysics 22, 309-344.

Griffiths, D.H. and King, R.F., 2013. *Applied geophysics for geologists and engineers: the elements of geophysical prospecting, pp. 1-5*. Elsevier.

Holden, J., Burt, T.P and Vilas, M. (2002). Application of ground-penetrating radar to the identification of subsurface piping in blanket peat. *Earth Surface Processes and Landforms*, *27*(3), pp.235-249

Hossain, M. S., Dharmateja, M., and Hossain, J. (2010). Assessment of geo-hazard potential and site investigations using Resistivity Imaging. International Journal of Environmental Technology and Management, 13(2), 116-129.

Isaksson, H., Thunehed, H., Pitkänen, T., and Keisu, M. (2007). Forsmark site investigation. Detailed ground magnetic survey and lineament interpretation in the Forsmark area, 2006-2007 (No. SKB-R--07-62). Swedish Nuclear Fuel and Waste Management Co.

Kearey, P., Brooks, M., and Hill, I. (2002). An introduction to geophysical exploration. John Wiley and Sons.

Lowe, J. and Zaccheo, P.F., 1991. Subsurface explorations and sampling. In *Foundation Engineering Handbook* (pp. 1-71). Springer, Boston, MA.

Mattsson, H., and Wahlgren, C. H. (2010). Interpretation of detailed ground magnetic data, resistivity and topographic data from Äspö (No. SKB-P--10-49). Swedish Nuclear Fuel and Waste Management Co.

Preprint not peer reviewed

This preprint research paper has not been peer reviewed. Electronic copy available at: https://ssrn.com/abstract=4072454

McDowell, P.W., Barker, R.D., Butcher, A.P., Culshaw, M.G., Jackson, P.D., McCann, D.M., Skipp, B.O., Matthews, S.L. and Arthur, J.C.R. (2002). *Geophysics in engineering investigations* (Vol. 19). London: Ciria.

Momoh, J. A., Xia, Y., and Boswell, G. D. (2008, September). An approach to determine Distributed Generation (DG) benefits in power networks. In 2008 40th North American Power Symposium (pp. 1-7). IEEE.

National Research Council. (2004). Groundwater fluxes across interfaces. National Academies Press

Oldham, C.H.G and Sutherland, D.B. (1955). Orthogonal polynomials, their used in the estimating the regional effect. Geophysics **20**, 295-306

Omatsola, M. E. and Adegoke, O. S. (1981). Tectonic evolution and Cretaceous stratigraphy of the Dahomey Basin. J. Min. Geol., 18, 130-137.

O'Neill, M. W. (2001). Side resistance in piles and drilled shafts. *Journal of Geotechnical and Geoenvironmental Engineering*, 127(1), 3-16.

Oni, A. G., Adediran, T. A., Olorunfemi, M. O., Eniola, P. J., and Adewale, E. A. (2020). Evaluation of the groundwater potential of Modomo Community in Ile-Ife, Southwest Nigeria, using integrated geophysical techniques. Sustainable Water Resources Management, 6(6), 1-18.

Oyedele, K. F., and Olorode, D. O. (2010). Site investigations of subsurface conditions using electrical resistivity method and cone penetration test at Medina Estate, Gbagada, Lagos, Nigeria.

Oyeniyi, T. O., Salami, A. A., and Ojo, S. B. (2016). Magnetic surveying as an aid to geological mapping: a case study from Obafemi Awolowo university campus in Ile-Ife, southwest Nigeria. Ife Journal of Science, 18(2), 331-343.

Preprint not peer reviewed

This preprint research paper has not been peer reviewed. Electronic copy available at: https://ssrn.com/abstract=4072454

Parsekian, A. D., Singha, K., Minsley, B. J., Holbrook, W. S. and Slater, L. (2015). Multiscale geophysical imaging of the critical zone. Reviews of Geophysics, 53(1), 1-26.

Paterson, N. R., and Reeves, C. V. (1985). Applications of gravity and magnetic surveys: The state-of-the-art in 1985. Geophysics, 50(12), 2558-2594.

Rana, S. (2019). Geophysical Investigations to Deal with Uncertainties in Difficult Ground Conditions. ISRM India Journal-Half Yearly Technical Journal of Indian National Group of ISRM, 8(2), 25-30.

Reid, A. B., Allsop, J. M., Granser, H., Millett, A. T., and Somerton, I. W. (1990). Magnetic interpretation in three dimensions using Euler deconvolution. Geophysics, 55(1), 80-91.

Reynolds, J. M. (1997): An Introduction to Applied and Environmental Geophysics 1997 John Wiley and Sons Ltd. New York.

Reynolds, J. M. (2011). An introduction to applied and environmental geophysics. John Wiley & Sons.

Ribes, D. and Finholt, T. A. (2009). The long now of infrastructure: Articulating tensions in development. Paul Edwards, Geoffrey C. Bowker, Steven Jackson, and Robin Williams (Eds). Volume 10, Special Issue 5, pp. 375-398.

Robinson, D. A., Binley, A., Crook, N., Day-Lewis, F. D., Ferré, T. P. A., Grauch, V. J. S., and Slater, L. (2008). Advancing process-based watershed hydrological research using near-surface geophysics: A vision for, and review of, electrical and magnetic geophysical methods. Hydrological Processes: An International Journal, 22(18), 3604-3635.

Salem, A., Williams, S., Fairhead, J. D., Ravat, D. and Smith, R. (2007). Tilt-depth method: A simple depth estimation method using first-order magnetic derivatives. The leading edge, 26(12), 1502-1505.

Telford, W. M., Telford, W. M., Geldart, L. P., and Sheriff, R. E. (1990). Applied geophysics. Cambridge university press.

Preprint not peer reviewed

This preprint research paper has not been peer reviewed. Electronic copy available at: https://ssrn.com/abstract=4072454

Udensi, E. E., and Osazuwa, I. B. (2004). Spectral determination of depths to magnetic rocks under the Nupe Basin, Nigeria. Nigerian Association of Petroleum Explorationists Bulletin, 17, 227.

USGS (2006) Shuttle radar topography mission, 1 Arc second scene, filled-finished-B, global land cover facility, Maryland: University of Maryland, College Park.

Verduzco, B., Fairhead, J. D., Green, C. M., and MacKenzie, C. (2004). New insights into magnetic derivatives for structural mapping. The leading edge, 23(2), 116-119.

Walters, K.A. (2008). Investigation of construction practices and test procedures for road pavements on expansive subgrades, pp. 1-331

Internet Resources

https://www.en.climate-data.org/africa/nigeria/lagos/lagos-552/ Retrieved on August, 2021.

https://www.lagosstate.gov.ng/about-lagos/ Retrieved on August, 2021.

Preprint not peer reviewed

This preprint research paper has not been peer reviewed. Electronic copy available at: https://ssrn.com/abstract=4072454